Bioorganic & Medicinal Chemistry 16 (2008) 10281–10294

Contents lists available at ScienceDirect

Bioorganic & Medicinal Chemistry

journal homepage: www.elsevier.com/locate/bmc

Structure–activity relationship studies of a new series of imidazo[2,1-*f*] purinones as potent and selective A_3 adenosine receptor antagonists

Pier Giovanni Baraldi [a,*], Delia Preti [a], Mojgan Aghazadeh Tabrizi [a], Romeo Romagnoli [a], Giulia Saponaro [a], Stefania Baraldi [a], Maurizio Botta [c], Cesare Bernardini [c], Andrea Tafi [c], Tiziano Tuccinardi [d], Adriano Martinelli [d], Katia Varani [b], Pier Andrea Borea [b]

[a] *Dipartimento di Scienze Farmaceutiche, Università di Ferrara, Via Fossato di Mortara 17-19, 44100 Ferrara, Italy*
[b] *Dipartimento di Medicina Clinica e Sperimentale-Sezione di Farmacologia, Università di Ferrara, 44100 Ferrara, Italy*
[c] *Dipartimento Farmaco Chimico Tecnologico, Università degli Studi di Siena, via A. Moro, 53100 Siena, Italy*
[d] *Dipartimento di Scienze Farmaceutiche, Università di Pisa, via Bonanno 6, 56126 Pisa, Italy*

ARTICLE INFO

Article history:
Received 26 May 2008
Revised 14 October 2008
Accepted 20 October 2008
Available online 1 November 2008

Keywords:
Adenosine
Cancer
A_3 antagonists
Imidazo[2,1-*f*]purinones
Docking
3D-QSAR

ABSTRACT

We recently described the synthesis of 1-benzyl-3-propyl-1*H*,8*H*-imidazo[2,1-*f*]purine-2,4-diones, new potent and selective A_3 adenosine receptor antagonists containing a xanthine core. The present work can be considered an extension of our SAR studies on related structures in which the effect of different kind of substitutions at the 1-, 3- and 8-positions has been evaluated in order to improve both the potency and the hydrophilicity of the originally synthesised molecules. The A_3 binding disposition of these compounds was also investigated through docking and 3D-QSAR studies.

1. Introduction

Adenosine regulates a number of physiological functions through the interaction with specific cell membrane G-protein coupled receptors ubiquitously expressed in the body and classified as A_1, A_{2A}, A_{2B} and A_3 (ARs).[1] The four known adenosine receptors subtypes, have been largely investigated thanks to their involvement in important pathologies.[2] The A_3 AR is able to inhibit forskolin-induced cAMP accumulation, to increase phosphatidylinositol-specific phospholipase C and D activity, and to elevate IP_3 levels and intracellular Ca^{2+} pools.[3] A_3 AR subtype has been subject of intensive investigations as potential therapeutic target due to its contribution to important pathophysiological processes such as inflammation,[4] neurodegeneration,[5,6] ischaemia,[7–9] asthma,[10,11] glaucoma[12–14] and cancer.[15–18] It has been suggested that adenosine inhibits tumour cell growth while maintaining bone marrow cell proliferation through the involvement of the A_3 receptors.[19] Studies related to a murine model demonstrated that the activation of A_3 receptors can interfere with the tumour cell recognition and with the cytolytic activity of cytotoxic lymphocytes, thus leading to the hypothesis that A_3 antagonists might be useful for the revelation of tumour-associated immunosuppression and facilitate adoptive immunotherapy.[15] Evidence of high levels of expression of A_3 adenosine receptor subtype has been provided in several tumour cell lines[20–23] and A_3 specific antagonists seem to synergistically enhance cytotoxic treatment and counter P-glycoprotein efflux in multi-drug resistance.[23] A recent study provides the first evidence that A_3 AR plays a role in colon tumorigenesis and, more importantly, can potentially be used as a diagnostic marker or a therapeutic target for colon cancer.[24]

Much effort has been directed toward searching for potent and selective human A_3 adenosine antagonists.[25–27] Some recent developments in this field comprise the identification of 1,2,4-triazolo[1,5-*i*]purines,[28] 1,2,4-triazolo[4,3-*a*]quinoxalin-1-ones,[29,30] thiazoles and thiadiazoles,[31,32] imidazo[2,1-*i*]purin-5-ones,[33] pyrido[2,1-*f*]purine-2,4-dione,[34] pyrazolo[3,4-*c*]/[4,3-*c*]quinolin-4-ones[35,36] and adenosine derivatives.[37–39] Generally, AR antagonists can be structurally classified into xanthine and non-xanthine derivatives, the first ones revealing, in most cases, low affinity toward A_3 receptor subtype. A useful strategy employed for the identification of adenosine receptors antagonists is the approach based on the annelation of xanthine derivatives.[40] Compounds characterized by the

* Corresponding author. Tel.: +39 0532 291293; fax: +39 0532 291296.
E-mail addresses: baraldi@dns.unife.it, brlpgv@unife.it, baraldi@unife.it (P.G. Baraldi).

0968-0896/$ - see front matter © 2008 Elsevier Ltd. All rights reserved.
doi:10.1016/j.bmc.2008.10.049

presence of fused rings on the xanthine nucleus have, in fact, shown different levels of affinity and selectivity to the various AR subtypes. During studies related to the identification of rigid analogues of KF17837, a known A_{2A} adenosine receptor antagonist belonging to the class of styryl xanthines, we synthesised and evaluated a series of 1,3-dipropyl-7-aryl/heteroaryl-1*H*,6*H*-pyrrolo[2,1-*f*]purine-2,4-diones[41] which did not show considerable affinity for the investigated targets. Subsequently, Priego et al. underlined the fundamental role of a benzyl and a propyl moieties at the 1- and 3-positions, respectively, of a series of 1*H*,3*H*-pyrido[2,1-*f*]purine-2,4-diones[34] examined as A_3 AR antagonists. In light of this we assumed that the lack of affinity of our reported 1,3-dipropyl-pyrrolo[2,1-*f*]purine-2,4-diones might be partially due to the presence of a propyl chain, instead of the benzyl moiety at the 1-position. We consequently performed the synthesis of a series of 7-aryl/alkyl-1*H*,6*H*-pyrrolo[2,1-*f*]purine-2,4-diones (see compounds **1m–p**[42] Table 1) and 7-aryl/alkyl-1*H*,8*H*-imidazo[2,1-*f*]purine-2,4-diones (see compounds **1a–l**[42] Table 1), evaluating in first instance the effect of the introduction of a benzyl and a propyl at the 1- and 3-position, respectively, in our previous series and in a new series of fused xanthine compounds.[42] Our attempt to introduce different kind of aryl and/or (cyclo)alkyl moieties at the 6- and 7-positions led us to identify very potent and selective A_3 adenosine receptors antagonists among which 1-benzyl-7-methyl-3-propyl-1*H*,8*H*-imidazo[2,1-*f*]purine-2,4-dione (**1a**,[42] Fig. 1) presents the best binding profile showing a K_i (hA_3) value from binding assay of 0.8 nM with considerable selectivity versus the other adenosine receptors subtypes (selectivity ratios of K_i (hA_1/hA_3) = 3163, K_i (hA_{2A}/hA_3) = 6250, IC_{50} (hA_{2B})/K_i (hA_3) = 2570). These compounds represent, to the best of our knowledge, the most potent and selective hA_3 adenosine receptor antagonists based upon a xanthine nucleus. In the present work we describe an extension of our reported series of imidazo-purinones performing new substitutions alternatively at the 1-, 3- and 8-positions of the reference compound **1a** (Fig. 1). Thanks to the identification of versatile synthetic routes we succeeded in manipulating the imidazo[2,1-*f*]purin-2,4-dione nucleus at various positions so to obtain the newly reported derivatives **6a–c**, **12**, **13**, **14a–f**, **15a–c**, **20a–b**, **24a–b** (Table 1) and to develop a SAR analysis combined with a molecular modeling study. Furthermore, on the basis of estimated *C*Log*P* values, the hydrophilicity of some of the new synthesized molecules has been improved in comparison with the reference compound **1a**.

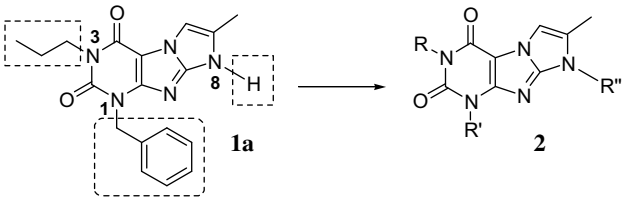

Figure 1. Substitution of the 1-, 3- and 8-positions of the imidazo[2,1-*f*]purine-2,4-diones.

2. Results and discussions

2.1. Chemistry

1-Benzyl-3-propyl-imidazo[2,1-*f*]purine-2,4-dione derivatives (**1a–l**, Table 1) and 1-benzyl-3-propyl-1*H*,6*H*-pyrrolo[2,1-*f*]purine-2,4-dione derivatives (**1m–p**) were prepared following the general synthetic strategy previously described.[42]

To realize final compounds **6a–c** bearing pyridyl-methyl moieties at the 1-position, the 3-benzyl-8-bromo-7-(2-oxo-propyl)-1-propyl-3,7-dihydro-purine-2,6-dione **3**[42] has been debenzylated[33] at the 3-position with anhydrous $AlCl_3$ in toluene (Scheme 1). Subsequent alkylation of **4** with 2/3/4-bromomethyl-pyridines and K_2CO_3 afforded the desired 3-substituted-intermediates **5a–c** which were cyclised in a steel bomb by treatment with liquid ammonia to the corresponding 7-methyl-3-propyl-1-pyridin-2/3/4-ylmethyl-1*H*,8*H*-imidazo[2,1-*f*]purine-2,4-diones **6a–c**. These were finally converted into the related hydrochloride salts via treatment with a saturated ethanolic solution of HCl.

1-Benzyl-3-(substituted)-7-methyl-1*H*,6*H*-pyrrolo[2,1-*f*]purine-2,4-diones (**12, 13 and 14a–f**), were prepared as depicted in Scheme 2. Bromination at the 8-position of 3-benzyl-3,7-dihydro-purine-2,6-dione[33] **7** by treatment with Br_2 and sodium acetate in acetic acid at 110 °C for 3 h[43] led to the formation of the 8-bromo-intermediate **8** with good yield. The following alkylation, occurring in presence of equimolar amounts of K_2CO_3 and α-chloroacetone in DMF at room temperature, permitted us to isolate with 70% yield, the N^7-2-oxo-propyl derivative **10**. The structural assignment was based on the knowledge that the distinctive resonance for the proton on the unsubstituted nitrogen at the 7-position was at about 13.5 ppm, while a broad singlet at about 11–12 ppm is the typical H–N^3/H–N^1 signal.[44] Carrying out the alkylation with an excess of 2 equiv of K_2CO_3 and 3 equiv of α-chloroacetone, it is possible to obtain the N^1,N^7-bis-(2-oxo-propyl) derivative **9**. The 3-benzyl-8-bromo-7-(2-oxo-propyl)-3,7-dihydro-purine-2,6-dione **10** was then treated with K_2CO_3 and the appropriate alkyl halide at room temperature, to furnish intermediates **11a–f**. The final tricycles **12**, **13** and **14a–f** were obtained by cyclisation of the corresponding intermediates **9**, **10** and **11a–f** which was performed according to the same conditions above described.

We identified intermediates **3** and **10** as suitable precursors for the obtainment of the 8-substituted-imidazo[2,1-*f*]purinones **15a–c** (Scheme 3) after treatment with triphenylphosphine and diethyl azodicarboxylate in the typical Mitsunobu reaction conditions.

The synthetic pathway illustrated in Scheme 4 permitted us to obtain final compounds **20a–b**. Refluxing **16a–b** in formic acid, fol-

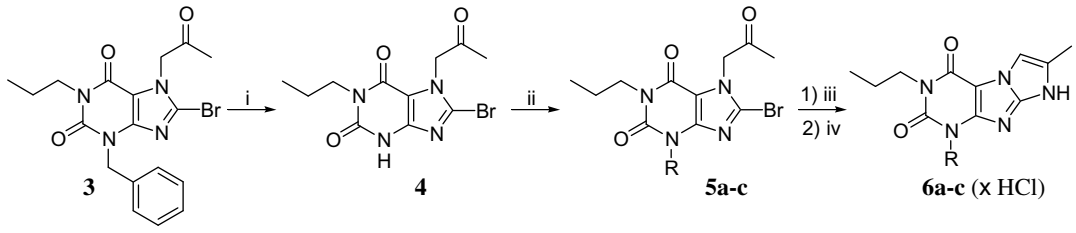

5a, 6a, 6a x HCl **R** = pyridin-4-ylmethyl
5b, 6b, 6bx HCl **R** = pyridin-3-ylmethyl
5c, 6c, 6c x HCl **R** = pyridin-2-ylmethyl

Scheme 1. Reagents and conditions: (i) $AlCl_3$, toluene, 1 h, 60 °C; (ii) 2/3/4-bromomethylpyridine, K_2CO_3, DMF, rt; (iii) NH_3, EtOH, ON, 100–120 °C; (iv) EtOH saturated with HCl, 30', rt.

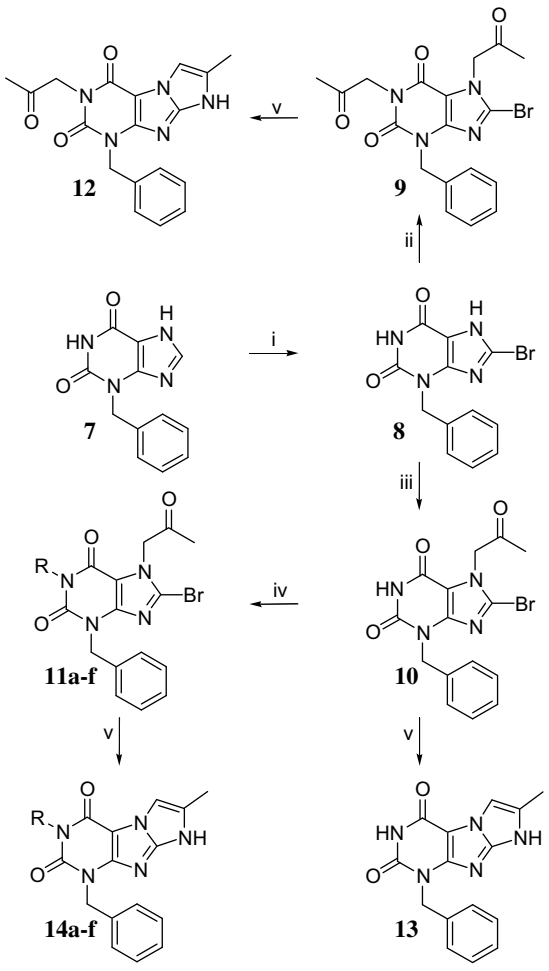

11a, 14a R = CH_2CH_2OH
11b, 14b R = $CH_2CH_2CH_2OH$
11c, 14c R = $CH_2CH{=}CH_2$
11d, 14d R = $CH_2C{\equiv}CH$
11e, 14e R = CH_2CO_2Et
11f, 14f R = $CH_2CH_2N(CH_3)_2$

Scheme 2. Reagents and conditions: (i) Br_2, CH_3COOH, 3 h, 110 °C; (ii) 3 equiv α-chloroacetone, 2 equiv K2CO3, DMF, rt; (iii) 1 equiv α-chloroacetone, 1 equiv K_2CO_3, DMF, rt; (iv) RX, K_2CO_3, DMF, rt; (v) NH3, EtOH, ON, 100–120 °C.

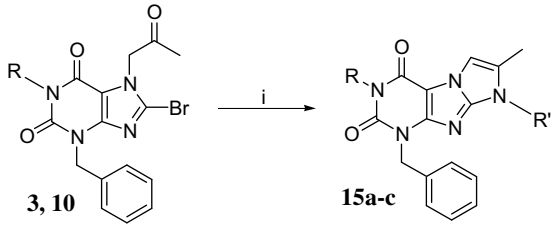

15a R = H; **R'** = 1-hydroxy-propyl-2-yl
15b R = H; **R'** = CH_2CH_3
15c R = $CH_2CH_2CH_3$; **R'** = CH_2CH_3

Scheme 3. Reagents and condition: (i) R'-NH_2, PPh3, DEAD, THF, 1 h, rt.

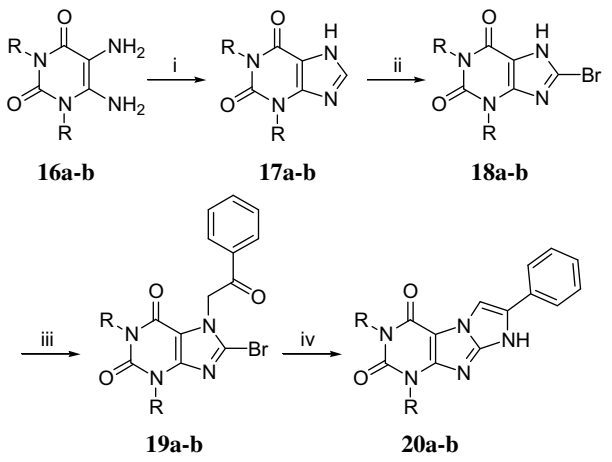

16-20a, **R** = propyl
16-20b, **R** = isobutyl

Scheme 4. Reagents and conditions: (i) a—HCO_2H, reflux, 1 h; b—NaOH, EtOH/H2O, reflux, 1 h; (ii) Br_2, CH_3CO_2H, CH_3CO_2Na, 45 °C, 1 h; (iii) α-Br-acetophenone, K_2CO_3, DMF, rt, 4 h; (iv) liquid ammonia, EtOH, 120 °C, ON.

lowed by treatment with NaOH in a mixture of EtOH and H_2O, induced the formation of 1,3-dialkyl-xanthines **17a–b** which were brominated at the 8-position (**18a–b**), alkylated at N^7 (**19a–b**) with α-bromoacetophenone and at last cyclised into the 1,3-dipropyl/diisobutyl-imidazo[2,1-*f*]purinones **20a–b** according to the synthetic steps describe for preparation of compound **13**. The 5,6-diamino-1,3-dipropyl/diisobutyl-1*H*-pyrimidine-2,4-dione derivatives **16a** and **16b** were obtained by the classical method reported in the literature, starting from the condensation of cyanoacetic acid and *N*,*N*′-dipropyl or *N*,*N*′-diisobutyl urea, followed by nitrosation at the 5-position and reduction of the nitroso group.[45]

Scheme 5 displays the preparation of compounds **24a–b**. 8-Nitro-theophylline[46] (**21**) was reduced by refluxing with hydrazine and 10% Pd/C in methanol to furnish intermediate **22**. This was alkylated with the corresponding α-bromoacetophenones at the N^7-position to obtain derivatives **23a–b**. The imidazole-ring closure was finally performed by refluxing **23a–b** in acetic acid to yield final tricycles **24a–b**.

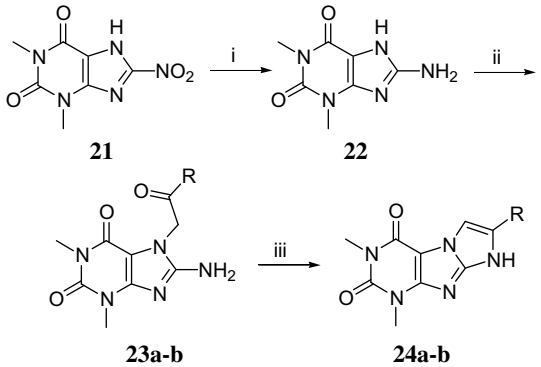

23-24a, **R** = Ph
23-24b, **R** = CH_3

Scheme 5. Reagents and conditions: (i) NH_2NH_2, 10% C/Pd, CH_3OH; (ii) α-haloketones, K_2CO_3, DMF, rt, 4–6 h; (iii) CH_3COOH, reflux, 4 h.

2.2. Biological evaluation and structure–affinity relationships

All the synthesized compounds (Table 1) were evaluated in radioligand binding assays to determine their affinities for human A_1, A_{2A}, and A_3 adenosine receptors. Potency of the compounds versus hA_{2B} adenosine receptors were studied evaluating their capability to inhibit (100 nM) NECA stimulated cAMP production. Basal and NECA stimulation of cAMP levels were 15 ± 2 and 80 ± 9 pmol cAMP/10^6 cells, respectively. NECA was able to stimulate cAMP levels in hA_{2B}CHO cells with an EC_{50} value of 145 ± 15 nM. Affinity data for A_1, A_{2A} and A_3 receptors, expressed as K_i values, and IC_{50} values derived from the cAMP assay carried out for hA_{2B} subtypes, are listed in Table 1.

With the previously reported series of compounds[42] (**1a–p**) we evaluated the effect of heterocycles fused on the N_7–C_8-positions of the xanthine nucleus. Among the examined tricycles, the imidazo[2,1-*f*]purine-2,4-dione derivatives were 2- to 10-fold more active than the corresponding substituted-pyrrolo[2,1-*f*]purine-2,4-dione derivatives toward the adenosine A_3 receptor subtype (compare **1a**, **1i** and **1g** to derivatives **1n**, **1m** and **1p**, respectively) with the only exception of compound **1o** which shows 4-fold higher hA_3 receptor affinity than the corresponding imidazo-purinone derivatives **1b**. The K_i (hA_3) values showed to be strictly dependent on the nature of the substituents at the 7-position. Our preliminary study indicated that the presence of a large aromatic and lipophilic moiety at the 7-position probably established repulsive interactions with the receptor, so we decided to evaluate the effect of replacing the aromatic nucleus with various (cyclo)alkyl chains. The best results were obtained with the introduction of a methyl group (**1a**, K_i (hA_3) = 0.8 nM with a surprising selectivity pattern vs the other AR subtypes). Attempt to introduce a substituent at the 6-position led to a loss of A_3 affinity. In light of these observations, in the newly synthesised series of imidazo[2,1-*f*]purine-2,4-dione derivatives, herein described, we generally decided to maintain the unsubstitution at the 6-position and the 7-methyl substitution (except for derivatives **20a–b** and **24a** functionalized at the 7-position with a phenyl ring) while investigating the effect of different kind of

Table 1
Binding, functional data and selectivity ratios at hA_1, hA_{2A}, hA_{2B}, and hA_3 adenosine receptors for the reported compounds

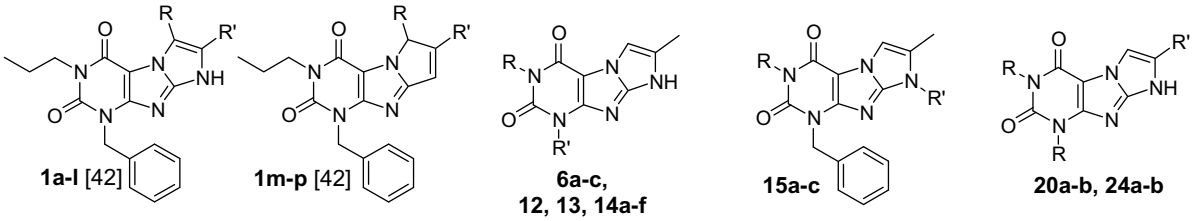

Compound	R	R'	hA_1[a]	hA_{2A}[b]	hA_{2B}[c]	hA_3[d]
1	H	CH_3	>1000	>1000	>1000	0.8 (0.6–0.9)
1b	H	CH_2CH_3	>1000	>1000	>1000	15 (9–27)
1c	H	$CH(CH_3)_2$	460 (424–498)	>1000	>1000	31 (25–38)
1d	H	$C(CH_3)_3$	>1000	>1000	>1000	99 (77–129)
1e	H	Cyclopropyl	350 (299–411)	>1000	>1000	23 (18–29)
1f	H	Cyclohexyl	>1000	>1000	>1000	555 (467–660)
1g	CH_3	CH_3	>1000	>1000	>1000	36 (31–43)
1h	CH_3	CH_2CH_3	>1000	>1000	>1000	60 (53–69)
1i	H	Ph	>1000	>1000	>1000	115 (89–150)
1j	H	4-OCH_3-Ph	>1000	>1000	>1000	55 (28–104)
1k	H	4-Ph-Ph	>1000	>1000	>1000	>1000
1l	H	4-F-Ph	>1000	>1000	>1000	22 (19–26)
1m	H	Ph	>1000	>1000	>1000	200 (134–297)
1n	H	CH_3	>1000	>1000	400 (323–496)	8.0 (7.1–9.1)
1o	H	CH_2CH_3	>1000	>1000	>1000	3.45 (2.71–4.36)
1p	CH_3	CH_3	>1000	>1000	>1000	80 (63–100)
6a × **HCl**	$CH_2CH_2CH_3$	pyridin-4-ylmethyl	>1000	>1000	>1000	141 (105–188)
6b × **HCl**	$CH_2CH_2CH_3$	pyridin-3-ylmethyl	>1000	>1000	>1000	57 (45–73)
6c × **HCl**	$CH_2CH_2CH_3$	pyridin-2-ylmethyl	>1000	>1000	>1000	34 (27–42)
12	CH_2COCH_3	CH_2Ph	>1000	>1000	>1000	182 (175–189)
13	H	CH_2Ph	>1000	>1000	>1000	148 (106–208)
14a	CH_2CH_2OH	CH_2Ph	>1000	>1000	>1000	38 (27–53)
14b	$CH_2CH_2CH_2OH$	CH_2Ph	>1000	>1000	>1000	110 (93–130)
14c	$CH_2CH=CH_2$	CH_2Ph	>1000	>1000	>1000	5.13 (3.93–6.70)
14d	$CH_2C{\equiv}CH$	CH_2Ph	>1000	>1000	>1000	15 (12–19)
14e	CH_2CO_2Et	CH_2Ph	>1000	>1000	>1000	20 (17–24)
14f	$CH_2CH_2N(CH_3)_2$	CH_2Ph	>1000	>1000	>1000	98 (81–119)
15a	H	1-hydroxy-propyl-2-yl	>1000	>1000	>1000	>1000
15b	H	CH_2CH_3	>1000	>1000	>1000	>1000
15c	$CH_2CH_2CH_3$	CH_2CH_3	>1000	>1000	>1000	200 (163–241)
20a	$CH_2CH_2CH_3$	Ph	373 (330–422)	>1000	>1000	99 (77–129)
20b	$CH_2CH(CH_3)_2$	Ph	476 (432–525)	>1000	>1000	144 (136–151)
24a	CH_3	Ph	>1000	>1000	>1000	>1000
24b	CH_3	CH_3	>1000	>1000	>1000	>1000

[a] Displacement of specific [^{3}H]-DPCPX binding to human A_1 receptors expressed in CHO cells (K_i nM, n = 4).
[b] Displacement of specific [^{3}H]-ZM 241385 binding to human A2A receptors expressed in CHO cells (K_i nM, n = 4).
[c] cAMP assay in CHO cells expressing hA2B receptors (IC_{50} nM, n = 4).
[d] Displacement of specific [^{3}H]-MRE3008F20 binding to human A_3 receptors expressed in CHO cells (K_i nM, n = 4). Binding and functional data of compounds **1a–p** from reference 42.

substituents at the 1-, 3- and 8-positions (see compounds **6a–c**, **12**, **13**, **14a–f**, **15a–c**, **24b**).

The substitution of the benzyl moiety at the 1-position with the pyridin-2/3/4-yl-methyl functions resulted in a substantial loss of affinity toward the A_3 adenosine receptor subtype. The comparison between the binding data of the reference compound **1a** (K_i (hA_3) = 0.8 nM) and the ones of the three hydrochloride salts of the 1-pyridyl isomer derivatives (**6a–c** × HCl) indicated that the presence of an heteroatom in the aromatic component induces a repulsive effect with the receptor binding site and that this effect becomes more evident when the nitrogen is exposed: K_i values progressively increase from the *ortho*- to the *meta*- to the *para*-isomer (**6c** × HCl K_i (hA_3) = 34 nM, **6b** × HCl K_i (hA_3) = 57 nM, **6a** × HCl K_i (hA_3) = 141 nM). These data induced us to suppose that the benzyl moiety could establish lipophilic interactions with a hydrophobic receptor pocket.

Removing the propyl chain at the 3-position of derivative **1a** determined a loss of 180-fold of affinity (**13**, K_i (hA_3) = 148 nM), while substitution at this position showed to be tolerated depending on the nature of the introduced function. Among these derivatives we identified compounds endowed with good A_3 affinity, such as the 2-hydroxy-ethyl derivative **14a** which has a K_i value of 38 nM and complete selectivity versus all the other adenosine receptor subtypes. The higher homologue **14b** resulted less potent (K_i (hA_3) = 110 nM). Satisfying results have been achieved constraining with unsaturations the conformations of the propyl chain at the 3-position of compound **1a**. The allyl (**14c**, K_i (hA_3) = 5 nM) and the propargyl (**14d**, K_i (hA_3) = 15 nM) derivatives resulted anyway 6- and 18-fold, respectively, less potent than **1a** in binding the hA_3 subtype.

With the synthesis of compounds **12** and **14e** it was possible to evaluate the effect of the substitution of the 3-propyl chain of **1a** with a moiety containing a carbonyl function. Although both the compounds resulted quite less potent than **1a** in binding the hA_3 receptor, the ethyl ester derivative **14e** (K_i (hA_3) = 20 nM) stands out as one of the most potent hA_3 ligand of the newly synthesised molecules.

To complete our SAR study of the reported tricyclic structures, we synthesized 1,3-dipropyl- (**20a**), 1,3-diisobutyl- (**20b**) and 1,3-dimethyl- (**24a–b**) derivatives in order to evaluate Priego's hypothesis regarding the primary role of 1-benzyl-3-propyl-substitution on the affinity of the A_3 receptor for our compounds. Replacement of the 1-benzyl moiety of **1i** with a propyl chain (**20a**) led to a substantial maintenance of A_3 receptor affinity, inducing at the same time a significant loss of selectivity versus adenosine hA_1 subtype. Compound **20b**, showing the symmetric substitution of N^1 and N^3-positions with isobutyl chains, displays a binding profile comparable to that of the dipropyl derivatives **20a** as it shows a reasonable hA_3 affinity (K_i hA_3 = 144 nM) but low selectivity versus the hA_1 subtype if compared with the remaining molecules of the series. According to Priego's results, 1,3-dimethyl-derivatives **24a–b** completely lose the capability to bind the four investigated receptor subtypes in comparison with the 1-benzyl-3-propyl-analogues **1i** and **1a**, respectively, confirming the fundamental contribution of the combination of the benzyl function at the 1-position with the propyl chain at the 3-position to the ligand-receptor binding. Since in an analogous manner, the introduction of a (substituted)-alkyl function at the 8-position determined a dramatically decrease of affinity of derivatives **15a–c**, the free ^{8}N–H seems to be fundamental for the ligand-receptor interaction.

Compounds **6c** (K_i (hA_3) = 34 nM) and **14a** (K_i (hA_3) = 38 nM), although less potent than **1a**, showed a good binding profile in association with enhanced hydrophilic properties on the basis of estimated *C*Log*P* values. The calculated Log*P* value of the starting compound **1a** (*C*Log*P* = 3.0 ± 1.38) resulted in effect higher then the calculated Log*P* values of compounds **6c** (*C*Log*P* = 1.51 ± 1.38) and **14a** (*C*Log*P* = 1.31 ± 1.39). All *C*Log*P* values have been determined with the version 7.0 of the ACD/Labs software.

2.3. Molecular modeling

Compound **1a**, which showed the highest affinity among the tested compounds (K_i = 0.8 nM), was docked into our previously reported A_3 receptor model (MODEL1) by means of AUTODOCK 3.0.[47] MODEL 1 was built through a ligand-aided homology procedure which made use of CATALYST program.[48]

The complex was then submitted to the optimizing protocol fully described in Section 4.

Compound **1a** was inserted between TM3, TM6 and TM7 with the *n*-propyl substituent directed towards the extracellular side of the receptor, the benzyl group towards the TM7 and the methyl substituent towards the intracellular side between TM3 and TM5.

More in details the imidazo[2,1-*f*]purine-2,4-dione central scaffold of compound **1a** was stabilized by π–π interactions with H95 and W243, and the 2-carbonyl group formed a H bond with N250. The 3-propyl group was inserted in a lipophilic pocket delimited by L91, I92, F182, and W185, the 1-benzyl group interacted with F239, L246, H272 and M276 while the 7-methyl group was stabilized by a lipophilic interaction with I98 and M99 (see Fig. 2).

This binding mode appeared to be in agreement with the mutagenesis studies, since the mutation of H95, W243, H272 and in particular N250 determined a reduction of the A3 antagonist affinity and in our model all these residues seemed to interact with the ligand.[49,50]

2.4. Automated docking analysis

All the other synthesized derivatives (compounds **1b–p**, **6a–c**, **12**, **13**, **14a–f**, **15a–c**, **20a–b** and **24a–b**) were docked by means of AUTODOCK 3.0[47] in the optimized A_3 receptor model obtained as previously described.

The docking analysis revealed that all the compounds with a K_i value lower than 100 nM showed a disposition very similar to the one found for **1a** which was characterized by: (a) an H bond between the 2-carbonyl group and N250, (b) the lipophilic interaction of the 1' substituent with F239, L246, H272 and M276, (c) the insertion of the 3-group in the lipophilic pocket delimited by L91, I92, F182, and W185.

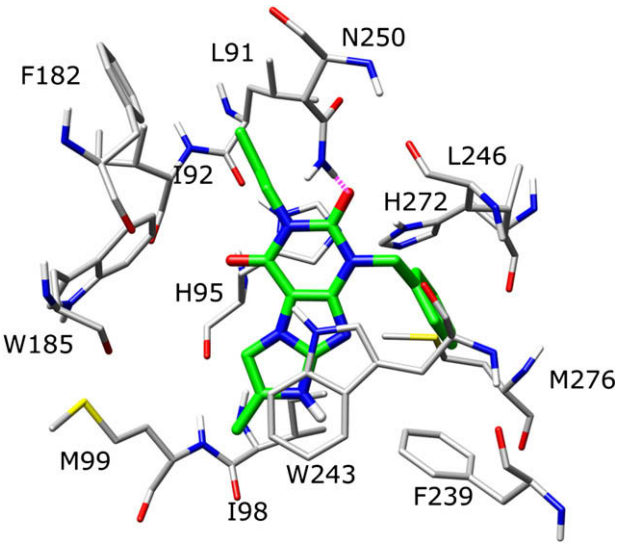

Figure 2. Compound **1a** docked in the A_3 binding site.

Compound **1l** (K_i = 22 nM) possessed the 4-F-phenyl substituent in 7-position. It maintained a disposition similar to that of compound **1a**, with only a slight shift of the ligand due to the presence of the bulky 4-F-phenyl group however allowing the formation of the H bond with N250 (see Fig. 3A). The substitution of the Fluorine atom with the methoxy group or with a hydrogen determined a decrease in A_3 affinity, however the docking studies were not able to explain this behaviour.

The substitution of the 4-F-phenyl with the biphenyl group resulted in a complete loss of A_3 affinity (compound **1k**, K_i >1000 nM). As shown in Figure 3B, this substituent was too bulky and determined the overturning of the ligand, with the loosing of the H bond with N250.

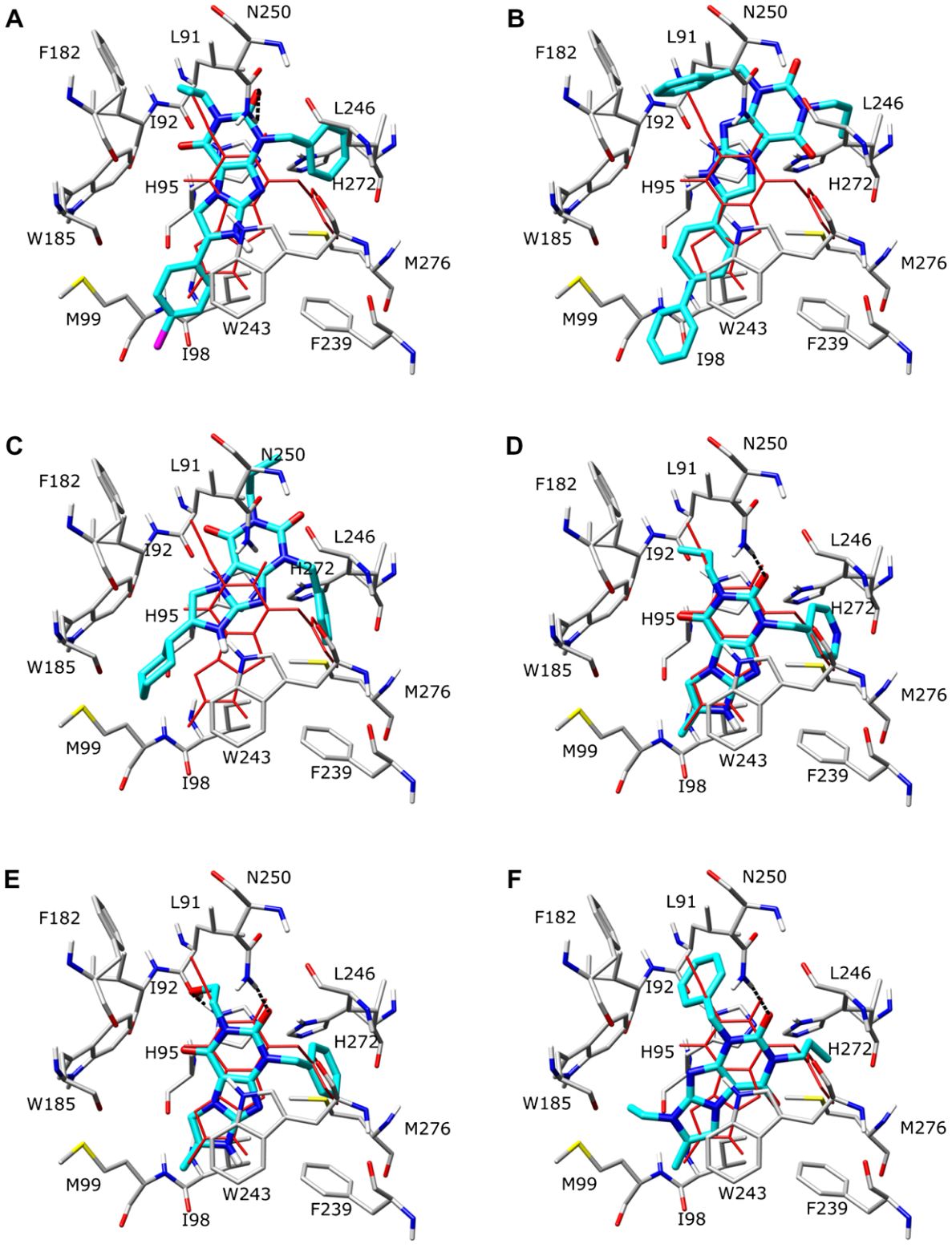

Figure 3. Compounds **1l**, **1k**, **1f**, **6a**, **14a** and **15c** docked into the A_3 receptor model.

Compound **1f** (K_i = 555 nM) possessed a bulky 7-cyclohexyl group that was not coplanar with the imidazo[2,1-*f*]purine-2,4-dione central scaffold and as shown in Figure 3C determining a large shift of the ligand with the losing of the H bond with N250.

The substitution of the 1-benzyl of **1a** with pyridinylmethyl groups (compound **6a–c**, K_i = 34–141 nM) resulted in a general decrease of the A_3 affinity and, as shown in Figure 3D that reported the analysis of compound **6a**, the docking studies showed for these groups the absence of any favourable electrostatic interaction with the receptor (see Fig. 3D).

A similar result was obtained also in the case of the 3-substitution: compounds **12**, **14b** and **14f**, which possessed a 3-group able to form H bonds, showed respect to **1a** a marked decrease of affinity and the docking analysis confirmed that these groups were unable to form any H bond with the receptor. The only exception was represented by compound **14a**, which possessed the 3-hydroxyethyl substituent able to interact with H95 (see Fig. 3E).

The alkylation of the N8 nitrogen determined a great decrease of affinity. The docking of compounds **15c**, suggested that the reason of this fact was not the lack of an H bond because this nitrogen seems to be unable to form any H bond with the receptor. It seems rather that the steric hindrance of the N substituents unable to occupy the very limited N8 region determined a completely different rearrangement of the central scaffold, with the N8 substituent pointing towards the extracellular side of the receptor, and the 1-benzyl substituent inserted in the lipophilic pocket delimited by L91, I92, F182, and W185 (see Fig. 3F).

2.5. 3D-QSAR analysis

With the aim of obtaining quantitative results that could support our binding hypothesis a 3D-QSAR analysis was carried out using the docking results as a receptor-based alignment.

The study was developed using three probes: the C3 (methyl) probe to account for steric contacts, the N2 = (sp^2 amide cation) and O (carbonylic oxygen) probes to evaluate the ability of each compound to be a hydrogen bond acceptor and donor respectively.[51] To measure the reliability of the 3D-QSAR model its correlation coefficient (r^2), predictive correlation coefficient (q^2) and cross-validated standard deviation of errors of prediction ($SDEP_{CV}$) were taken into consideration.

Another 3D-QSAR model was developed using a ligand-based alignment, that is, by aligning the central scaffold of all the 34 compounds.

As shown in Table 2 the model obtained using the ligand-based alignment did not display good results, whereas the model obtained by means of the receptor-based alignment showed good results, since the r^2, q^2 and $SDEP_{CV}$ were respectively 0.91, 0.67, and 0.42.

The plot reporting the experimental versus the calculated affinity of model 2 highlighted that the 3D-QSAR model was capable of well predicting the affinity of all compounds with only the exception of **1a** for which an affinity approximately 20-fold lower than the experimental one was calculated (see Fig. 4).

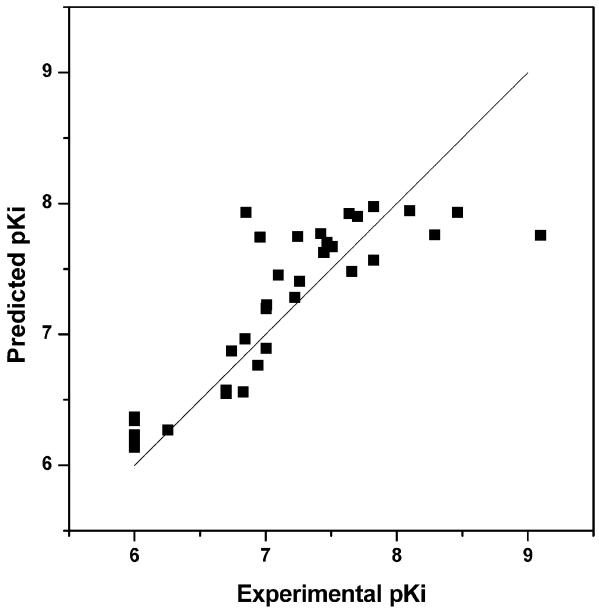

Figure 4. Plot of model 2 (four principal components): experimental/predicted pK_i is reported.

One important feature of 3D-QSAR analysis is the graphic representation of the model, usually aimed at making its interpretation easier. In the GOLPE program,[52] there are several options for displaying the final model. Among these, the PLS pseudo coefficient is very useful because it makes possible to visualise favourable and unfavourable interactions between the probes and the studied molecules.

Figure 5 shows compound **1o** embedded in the contour maps of the C3 probe and the sterically favoured (yellow) and unfavoured (cyan) regions were indicated; in particular there were three principal regions (A–C) with positive values (see Fig. 5a) in which a favourable interaction between a substituent and the probe determined an increase in activity, whereas an unfavourable interaction between a substituent and the probe determined a decrease in activity. On the contrary, the negative PLS coefficients, indicated in Figure 5b, show three main areas (A'–C') where a favourable interaction between a substituent and the probe determined a decrease in activity, whereas an unfavourable interaction between a substituent and the probe determined an increase in activity.

The analysis of these maps suggested that the favourable regions A and C, corresponding to the two lipophilic pockets, delim-

Table 2
Statistical results of the 3D-QSAR models. In bold is reported the optimal dimensionality.

PC	Ligand-based 3D-QSAR model (Var = 1888)			Receptor Based 3D-QSAR model (Var = 1674)		
	Model 1			Model 2		
	r^2	q^2	$SDEP_{cv}$	r^2	q^2	$SDEP_{cv}$
1	0.54	0.34	0.60	0.52	0.39	0.57
2	0.61	0.38	0.58	0.77	0.57	0.48
3	**0.73**	**0.40**	**0.57**	0.86	0.66	0.43
4	0.78	0.40	0.57	**0.91**	**0.67**	**0.42**
5	0.79	0.37	0.58	0.92	0.64	0.44

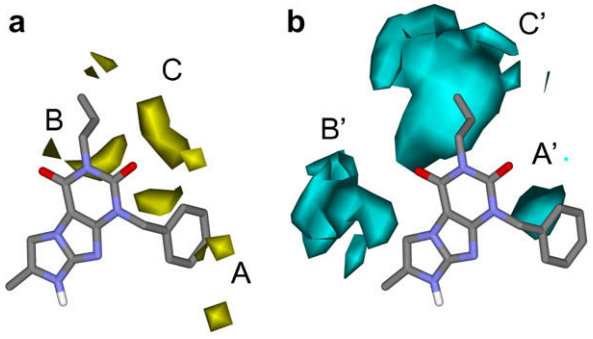

Figure 5. Positive (a) and negative (b) regions of the PLS coefficient plot obtained with the C3 probe. Compound **14c** is also displayed.

ited by F239, L246, H272 and M276 and L91, I92, F182, and W185, respectively, were important for the affinity, however the unfavourable regions A' and C' seemed to indicate that too bulky substituents were not allowed.

The region B corresponded to the π–π interaction between the central scaffold and H95 and the region B' corresponded to W185, and, as shown by the docking of compounds **15a–c** (see Fig. 3F), a substituent in this region determined a decrease of affinity.

The contour maps of the N2= and O (see Fig. 6) were very similar, the positive region (regions A of Fig. 6b and d) for which a favourable interaction between a substituent and these probes determined a decrease in activity, were positioned in the same portion of space as region A of the C3 probe thus confirming that this region should possess a lipophilic characteristic in order to improve the ligand affinity. As regards the negative regions (Fig. 6a and c), there was only one region (A') corresponding to the electrostatic interaction of the hydroxymethyl substituent of compound **14a** with H95.

3. Conclusion

Herein we evaluated the effect of different kind of substitutions at the 1-, 3-and 8-positions of the reference compound 1-benzyl-7-methyl-3-propyl-1*H*,8*H*-imidazo[2,1-*f*]purine-2,4-dione **1a**, Figure 1[42] Some of the new reported compounds confirmed high A_3 AR binding affinity in association with relevant selectivity versus the remaining ARs (**14c**, K_i (hA_3) = 5.13 nM, (hA_1–hA_{2A}–hA_{2B}/hA_3) >195; **14d**, K_i (hA_3) = 15 nM, (hA_1-hA_{2A}-hA_{2B}/hA_3) >67). Compounds **6c** × HCl (K_i (hA_3) = 34 nM) and **14a** (K_i (hA_3) = 38 nM), although less potent than **1a**, showed a good binding profile in association with enhanced hydrophilic properties on the basis of estimated *C*Log*P* values.

The binding disposition of these molecules was investigated by means of a docking approach using the mixed pharmacophoric-molecular modeling procedure and the A_3 receptor model previously reported.[48] The obtained results highlighted the interaction of these compounds with the main residues suggested to be important by mutagenesis studies.

Furthermore the docking poses were used as an alignment tool for the generation of a 3D-QSAR model which was able to quantitative explain the different affinity of the ligands.

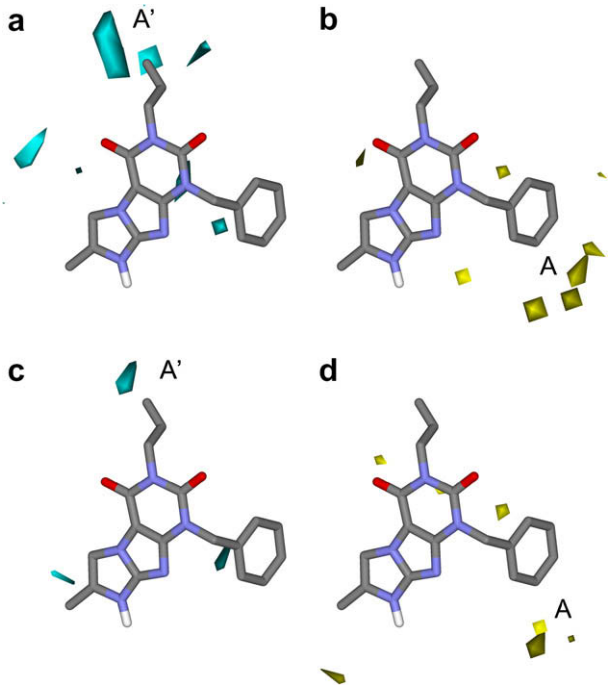

Figure 6. Negative (a, c) and positive (b,d) regions of the PLS coefficient plot obtained with the N2= (a,b) and O (c,d) probe. Compound **14c** is also displayed.

4. Experimental

4.1. Chemistry

Reaction progress and product mixtures were monitored by thin-layer chromatography (TLC) on silica gel (procoated F_{254} Merck plates) and visualized with aqueous potassium permanganate or a methanolic solution of ninhydrin. ^{1}H NMR were determined in $CDCl_3$ or DMSO-d_6 solutions with a Varian VXR 200 spectrometer or a Varian Mercury Plus 400 spectrometer; peak positions are given in parts per million (δ) downfield from tetramethylsilane as internal standard and *J* values are given in Hertz. Light petroleum refers to the fractions boiling at 40–60 °C. Melting points were determined on a Buchi–Tottoli instrument and are uncorrected. Chromatography was performed on Merck 230–400 mesh silica gel. Organic solutions were dried over anhydrous sodium sulphate. Elemental analyses were performed by the microanalytical laboratory of Dipartimento di Chimica, University of Ferrara, and were within ± 0.4% of the theoretical values for C, H and N.

4.1.1. 8-Bromo-7-(2-oxo-propyl)-1-propyl-3,7-dihydro-purine-2,6-dione (4)

A solution of **3**[42] (0.48 mmol) in anhydrous toluene (5 mL) was stirred under argon atmosphere at room temperature and anhydrous $AlCl_3$ (2.4 mmol) was added. The reaction was heated for 1 h at 60 °C. The solvent was evaporated and the residue partitioned between H_2O (20 mL) and EtOAc (3× 30 mL). The combined organic layers were dried on Na_2SO_4, filtered and the solvent evaporated to furnish a residue which was crystallized with a mixture of Et_2O/light petroleum 1:1 (20 mL). The solid was filtered, washed with light petroleum and dried under vacuum. Yield 76%, white solid; mp 244–245 °C; ^{1}H NMR (DMSO-d_6, 400 MHz) δ (ppm): 0.82 (t, 3H, *J* = 7.4), 1.50 (m, 2 H), 2.49 (s, 3H), 3.72 (t, 2H, *J* = 7.5), 5.23 (s, 2H), 12 (br s, 1H).

4.1.2. General procedure for the synthesis of 8-bromo-7-(2-oxo-propyl)-1-propyl-3-pyridin-2/3/4-ylmethyl-3,7-dihydro-purine-2,6-dione derivatives (5a–c)

To a solution of **4** (0.3 mmol) in anhydrous DMF (3 mL), K_2CO_3 was added (0.6 mmol) and the resulting suspension was stirred at room temperature for 1 h. After cooling at 0 °C a solution of the appropriate alkyl halide (0.33 mmol) in DMF (2 mL) was added dropwise. The reaction proceeded under stirring at 0 °C for 5' and at room temperature for further 50'. The solvent was evaporated under vacuum to obtain a residue which was suspended with H_2O, acidified with a 5% aqueous solution of HCl and extracted with EtOAc (2× 20 mL). The aqueous phase was then basified with NaOH 5% and extracted a second time with EtOAc (3× 20 mL). The second organic layer was dried on Na_2SO_4, filtered and the solvent was evaporated under vacuum till dryness.

4.1.3. 8-Bromo-7-(2-oxo-propyl)-1-propyl-3-pyridin-4-ylmethyl-3,7-dihydro-purine-2,6-dione (5a)

The product was purified by column chromatography on silica gel (EtOAc/light petroleum 7:3). Yield 60%, white solid; mp 118–120 °C; ^{1}H NMR (DMSO-d_6, 400 MHz): δ (ppm) 0.83 (t, 3H, *J* = 7.2), 1.53 (m, 2H), 2.30 (s, 3H), 3.79 (m, 2H), 5.17 (s, 2H), 5.30 (s, 2H), 7.26 (dd, 2H, *J* = 8), 8.51 (dd, 2H, *J* = 8).

4.1.4. 8-Bromo-7-(2-oxo-propyl)-1-propyl-3-pyridin-3-ylmethyl-3,7-dihydro-purine-2,6-dione (5b)

The product was purified by column chromatography on silica gel (EtOAc/light petroleum 7:3). Yield 75%, white solid; mp 154 °C; ^{1}H NMR (DMSO-d_6, 200 MHz): δ (ppm) 0.81 (t, 3H, J = 7.6), 1.50 (m, 2H), 2.27 (s, 3H), 3.76 (m, 2H), 5.15 (s, 2H), 5.26 (s, 2H), 7.32–7.38 (m, 1H), 7.68–7.74 (m, 1H), 8.46 (m, 1H), 8.56 (m, 1H).

4.1.5. 8-Bromo-7-(2-oxo-propyl)-1-propyl-3-pyridin-2-ylmethyl-3,7-dihydro-purine-2,6-dione (5c)

The product was purified by column chromatography on silica gel (EtOAc/light petroleum 7:3). Yield 65%, white solid; mp 160 °C; ^{1}H NMR (DMSO-d_6, 200 MHz): δ (ppm) 0.80 (t, 3H, J = 7.5), 1.48 (m, 2H), 2.27 (s, 3H), 3.76 (m, 2H), 5.22 (s, 2H), 5.28 (s, 2H), 7.22–7.31 (m, 2H), 7.71–7.79 (m, 1H), 8.42–8.45 (m, 1H).

4.1.6. General procedure for the synthesis of the final 7-methyl-3-propyl-1-pyridin-(2/3/4)-ylmethyl-1*H*,8*H*-imidazo[2,1-*f*]purine-2,4-dione derivatives (6a–c)

The appropriate 8-bromo-7-(2-oxo-propyl)-3,7-dihydro-purine-2,6-dione derivatives **5a–c** (0.4 mmol) was dissolved in EtOH (4 mL) and liquid ammonia (2–3 mL) was added. The reaction was heated at 100–120 °C in a steel bomb overnight. The solvent was evaporated till dryness.

4.1.7. 7-Methyl-3-propyl-1-pyridin-4-ylmethyl-1*H*,8*H*-imidazo-[2,1-*f*]purine-2,4-dione (6a)

The product was purified by column chromatography on silica gel (CH_2Cl_2/CH_3OH 9.5:0.5). Yield 40%, white solid; mp 275 °C; ^{1}H NMR (DMSO-d_6, 400 MHz): δ (ppm) 0.86 (t, 3H, J = 7.6), 1.56 (m, 2H), 2.26 (s, 3H), 3.84 (m, 2H), 5.18 (s, 2H), 7.26 (m, 3H), 8.48 (d, 2H, J = 6), 12.30 (br s, 1H).

4.1.8. 7-Methyl-3-propyl-1-pyridin-3-ylmethyl-1*H*,8*H*-imidazo-[2,1-*f*]purine-2,4-dione (6b)

The product was purified by column chromatography on silica gel (EtOAc/CH_3OH 9.5:0.5). Yield 50%, white solid; 280 °C dec.; ^{1}H NMR (DMSO-d_6, 200 MHz): δ (ppm) 0.83 (t, 3H, J = 7.2), 1.53 (m, 2H), 2.23 (s, 3H), 3.82 (m, 2H), 5.24 (s, 2H), 7.16–7.26 (m, 3H), 7.65–7.40 (m, 1H), 8.42 (m, 1H), 12.30 (br s, 1H).

4.1.9. 7-Methyl-3-propyl-1-pyridin-2-ylmethyl-1*H*,8*H*-imidazo-[2,1-*f*]purine-2,4-dione (6c)

The product was purified by column chromatography on silica gel (EtOAc/CH_3OH 9.5:0.5). Yield 80%, white solid; mp 285 °C; ^{1}H NMR (DMSO-d_6, 200 MHz): δ (ppm) 0.82 (t, 3H, J = 7.2), 1.53 (m, 2H), 2.24 (s, 3H), 3.81 (m, 2H), 5.16 (s, 2H), 7.21–7.34 (m, 2H), 7.69–7.74 (m, 1H), 8.44 (m, 1H), 8.58 (m, 1H), 12.30 (br s, 1H).

4.1.10. General procedure for the synthesis of the hydrochlorides salts of compounds (6a–c)

The appropriate tricyclic derivative **6a–c** as a free base (0.1 mmol), was suspended in a saturated ethanolic solution of HCl. The mixture was stirred at room temperature for 30', then the solvent was evaporated and the residue coevaporated for three times with Et_2O. The hydrochloride salts were purified via crystallization from EtOH.

4.1.11. 8-Bromo-7-(2-oxo-propyl)-1-propyl-3-pyridin-4-ylmethyl-3,7-dihydro-purine-2,6-dione hydrochloride (6a × HCl)

Yield 90%, white solid; mp >300 °C; ^{1}H NMR (DMSO-d_6, 200 MHz): δ (ppm) 0.86 (t, 3H, J = 7.2), 1.57 (m, 2H), 2.27 (s, 3H), 3.84 (m, 2H), 5.39 (s, 2H), 7.29 (s, 1H), 7.80 (d, 2H, J = 6), 8.75 (d, 2H, J = 6), 12.32 (s, 1H).

4.1.12. 8-Bromo-7-(2-oxo-propyl)-1-propyl-3-pyridin-3-ylmethyl-3,7-dihydro-purine-2,6-dione hydrochloride (6b × HCl)

Yield 95%, white solid; 300 °C dec.; ^{1}H NMR (DMSO-d_6, 200 MHz): δ (ppm) 0.85 (t, 3H, J = 7.2), 1.58 (m, 2H), 2.27 (s, 3H), 3.82 (m, 2H), 5.31 (s, 2H), 7.27 (s, 1H), 7.80 (m, 1H), 8.26 (m, 1H), 8.70–8.83 (m, 2H), 12.37 (s, 1H).

4.1.13. 8-Bromo-7-(2-oxo-propyl)-1-propyl-3-pyridin-2-ylmethyl-3,7-dihydro-purine-2,6-dione hydrochloride (6c × HCl)

Yield 90%, white solid; mp >300 °C; ^{1}H NMR (DMSO-d_6, 200 MHz): δ (ppm) 0.85 (t, 3H, J = 7.2), 1.55 (m, 2H), 2.26 (s, 3H), 3.87 (m, 2H), 5.35 (s, 2H), 7.27 (s, 1H), 7.45 (m, 2H), 7.95 (m, 1H), 8.56 (m, 1H), 12.26 (s, 1H).

4.1.14. 3-Benzyl-8-bromo-3,7-dihydro-purine-2,6-dione (8)

A mixture of 3-benzyl-xanthine **7**[32] (16.5 mmol) and anhydrous CH_3CO_2Na (33 mmol) in AcOH (90 mL) was heated under stirring at 110 °C, then Br_2 was added (16.5 mmol). The reaction proceeded at the same temperature for 3 h. The solvent was evaporated and the residue was suspended with cold water and cooled at 0 °C. The product was filtered, washed with cold water and dried under vacuum. Yield 80% white solid; mp 287–289 °C; ^{1}H NMR (DMSO-d_6, 200 MHz) δ (ppm): 5.06 (s, 2H), 7.19–7.36 (m, 5H), 11.28 (s, 1H), 14.38 (br s, 1H).

4.1.15. 3-Benzyl-8-bromo-1,7-bis-(2-oxo-propyl)-3,7-dihydro-purine-2,6-dione (9)

The 8-bromo-3-benzyl-xanthine **8** (3.11 mmol) was dissolved in anhydrous DMF (4 mL) and Na_2CO_3 (0.66 g, 6.22 mmol) was added to the solution. A solution of α-chloro-acetone (9.33 mmol) in anhydrous DMF (2 mL) was then added dropwise within 1 h. The reaction was stirred at room temperature overnight. The solvent was evaporated and the residue was partitioned between H_2O (30 mL) and CH_2Cl_2 (3 × 50 mL). The organic layer was dried on anhydrous Na_2SO_4, filtered the solvent was evaporated to give a residue which was purified by crystallization with a mixture of CH_2Cl_2/light petroleum 1:2. Yield 88% white solid; mp 248–250 °C; ^{1}H NMR (DMSO-d_6, 200 MHz) δ (ppm): 2.17 (s, 3H), 2.26 (s, 3H), 4.71 (s, 2H), 5.13 (s, 2H), 5.26 (s, 2H), 7.31 (m, 5H).

4.1.16. 3-Benzyl-8-bromo-7-(2-oxo-propyl)-3,7-dihydro-purine-2,6-dione (10)

The product was prepared according to the procedure described for the synthesis of **9** but reacting the 8-bromo-3-benzyl-xanthine (3.11 mmol) with 3.11 mmol of Na_2CO_3 and 3.11 mmol of α-chloro-acetone. Yield 70% white solid; mp 207–209 °C; ^{1}H NMR (DMSO-d_6, 200 MHz) δ (ppm): 2.26 (s, 3H), 5.06 (s, 2H), 5.23 (s, 2H), 7.31 (m, 5H), 11.47 (br s, 1H).

4.1.17. General procedure for the preparation of 3-benzyl-8-bromo-1-substituted-7-(2-oxo-propyl)-3,7-dihydro-purine-2,6-dione derivatives (11a–f)

A solution of **10** (0.40 mmol) in anhydrous DMF (2 mL) was stirred at room temperature and K_2CO_3 (0.40 mmol) was added. After 5' a solution of the appropriate alkyl halides (0.80 mmol), in DMF (2 mL), was slowly added dropwise. The reaction was stirred at room temperature and monitored with TLC (2–5 h). The solvent was evaporated to obtain a residue which was suspended with CH_2Cl_2 (20 mL) and washed with H_2O (2× 10 mL). The organic phase was dried on anhydrous Na_2SO_4, filtered and the solvent was evaporated till dryness.

4.1.18.3-Benzyl-8-bromo-1-(2-hydroxy-ethyl)-7-(2-oxo-propyl)-3,7-dihydro-purine-2,6-dione (11a)

The intermediate was purified via crystallization with a mixture of Et_2O/light petroleum 1:2. Yield 70% white solid; mp 143–

144 °C; ^{1}H NMR (DMSO-d_6, 200 MHz): δ (ppm) 2.29 (s, 3H), 3.49 (m, 2H), 3.92 (m, 2H), 4.77 (bt, 1H), 5.13 (s, 2H), 5.29 (s, 2H), 7.33 (m, 5H).

4.1.19. 3-benzyl-8-bromo-1-(3-hydroxy-propyl)-7-(2-oxo-propyl)-3,7-dihydro-purine-2,6-dione (11b)

The product was purified by column chromatography on silica gel (CH_2Cl_2/CH_3OH 9.9:0.1). Yield 65%, colourless oil; ^{1}H NMR (DMSO-d_6, 200 MHz): δ (ppm) 1.81 (m, 2H), 2.32 (s, 3H), 3.46 (t, 2H), 4.09 (t, 2H), 5.15 (s, 2H), 5.22 (s, 2H), 7.25–7.50 (m, 5H).

4.1.20. 1-Allyl-3-benzyl-8-bromo-7-(2-oxo-propyl)-3,7-dihydro-purine-2,6-dione (11c)

The product was purified by column chromatography on silica gel (CH_2Cl_2/CH_3OH 9.8:0.2): Yield 80%, white solid; mp 145 °C; ^{1}H NMR (DMSO-d_6, 400 MHz): δ (ppm) 2.28 (s, 3H), 4.43 (d, 2H, J = 2.6), 5.07 (m, 2H), 5.14 (s, 2H), 5.29 (s, 2H), 5.80 (m,1H), 7.34 (m, 5H).

4.1.21. 3-Benzyl-8-bromo-7-(2-oxo-propyl)-1-prop-2-ynyl-3,7-dihydro-purine-2,6-dione (11d)

The intermediate was purified via crystallization with a mixture of Et_2O/light petroleum 1:2: Yield 77%, brown solid; mp 147 °C; ^{1}H NMR (DMSO-d_6, 200 MHz): δ (ppm) 2.16 (m, 1H), 2.34 (s, 3H), 4.70 (d, 2H, J = 2.4), 5.17 (s, 2H), 5.25 (s, 2H), 7.29–7.40 (m, 3H), 7.51–7.56 (m, 2H).

4.1.22. [3-Benzyl-8-bromo-2,6-dioxo-7-(2-oxo-propyl)-2,3,6,7-tetrahydro-purin-1-yl]-acetic acid ethyl ester (11e)

The intermediate was purified via crystallization with a mixture of Et_2O/light petroleum 1:2. Yield 62%, pale yellow solid; mp 174–176 °C; ^{1}H NMR (DMSO-d_6, 200 MHz): δ (ppm) 1.16 (t, 3H, J = 7.3), 2.28 (s, 3H), 4.10 (q, 2H, J = 7.3), 4.59 (s, 2H), 5.16 (s, 2H), 5.29 (s, 2H), 7.32 (m, 5H).

4.1.23. 3-Benzyl-8-bromo-1-(2-dimethylamino-ethyl)-7-(2-oxo-propyl)-3,7-dihydro-purine-2,6-dione (11f)

The intermediate was purified via crystallization with a mixture of Et_2O/light petroleum 1:2: Yield 70%, white solid; mp 130–131 °C; ^{1}H NMR (DMSO-d_6, 400 MHz): δ (ppm) 2.16 (s, 6H), 2.30 (s, 3H), 2.40 (t, 2H, J = 7.2), 3.90 (t, 2H, J = 7.2), 5.17 (s, 2H), 5.30 (s, 2H), 7.40 (m, 5H).

4.1.24. General procedure for the synthesis of the final 1-benzyl-3-substituted-7-methyl-1*H*,8*H*-imidazo[2,1-*f*]purine-2,4-dione derivatives (12, 13, 14a–f)

The appropriate 8-bromo-7-(2-oxo-propyl)-3,7-dihydro-purine-2,6-dione derivatives (**9, 10, 11a–f**) (0.4 mmol) was dissolved in EtOH (4 mL) and liquid ammonia (2–3 mL) was added. The reaction was heated at 100–120 °C in a steel bomb overnight. The solvent was evaporated till dryness.

4.1.25. 1-Benzyl-7-methyl-3-(2-oxo-propyl)-1*H*,8*H*-imidazo-[2,1-*f*]purine-2,4-dione (12)

The product was crystallized from EtOAc. Yield 85%, white solid; mp 280–282 °C; ^{1}H NMR (DMSO-d_6, 200 MHz): δ (ppm) 2.17 (s, 3H), 2.25 (s, 3H), 4.72 (s, 2H), 5.15 (s, 2H), 7.23–7.31 (m, 6H), 12.00 (br s, 1H).

4.1.26. 1-Benzyl-7-methyl-1*H*,3*H*,8*H*-imidazo[2,1-*f*]purine-2,4-dione (13)

The product was crystallized from a mixture of CH_3OH/H_2O 1:1. Yield 75%, white solid; mp >300 °C; ^{1}H NMR (DMSO-d_6, 200 MHz): δ (ppm) 2.25 (s, 3H), 5.09 (s, 2H), 7.23–7.32 (m, 6H), 10.95 (br s, 1H), 13.00 (br s, 1H).

4.1.27. 1-Benzyl-7-methyl-3-(2-hydroxy-ethyl)-1*H*,8*H*-imidazo[2,1-*f*]purine-2,4-dione (14a)

The product was purified by column chromatography on silica gel (CH_2Cl_2/CH_3OH 9.5:0.5). Yield 60%, white solid; mp 257–259 °C; ^{1}H NMR (DMSO-d_6, 200 MHz): δ (ppm) 2.50 (s, 3H), 3.52 (t, 2H, J = 6.6), 3.97 (t, 2H, J = 6.6), 4.9 (br s, 1H), 5.15 (s, 2H), 7.23–7.33 (m, 6H), 12.30 (br s, 1H).

4.1.28. 1-Benzyl-7-methyl-3-(2-hydroxy-propyl)-1*H*,8*H*-imidazo-[2,1-*f*]purine-2,4-dione (14b)

The product was purified by column chromatography on silica gel (CH_2Cl_2/CH_3OH 9.5:0.5). Yield 70%, white solid; mp 259–260 °C; ^{1}H NMR (DMSO-d_6, 200 MHz): δ (ppm) 1.69 (m, 2H), 2.26 (s, 3H), 3.43 (m, 2H), 3.93 (t, 2H), 4.40 (bt, 1H), 5.16 (s, 2H), 7.24–7.33 (m, 6H), 12.20 (br s, 1H).

4.1.29. 1-Benzyl-7-methyl-3-allyl-1*H*,8*H*-imidazo[2,1-*f*]purine-2,4-dione (14c)

The product was crystallized from a mixture of CH_3OH/H_2O 1:1. Yield 70%, white solid; mp 258–260 °C; ^{1}H NMR (DMSO-d_6, 200 MHz): δ (ppm) 2.23 (s, 3H), 4.45 (d, 2H, J = 4), 4.97 (m, 2H), 5.13 (s, 2H), 5.82 (m, 1H), 7.21–7.33 (m, 6H), 12.00 (br s, 1H).

4.1.30. 1-Benzyl-7-methyl-3-prop-2-ynyl-1*H*,8*H*-imidazo[2,1-*f*]purine-2,4-dione (14d)

The product was purified by column chromatography on silica gel (CH_2Cl_2/CH_3OH 9.5:0.5). Yield 60%, white solid; mp 248–249 °C; ^{1}H NMR (DMSO-d_6, 200 MHz): δ (ppm) 2.22 (s, 3H), 4.57 (d, 2H, J = 2), 5.13 (s, 2H), 7.20–7.33 (m, 6H), 12.20 (br s, 1H).

4.1.31. (1-Benzyl-7-methyl-2,4-dioxo-1,2,4,8-tetrahydro-imidazo-[2,1-*f*]purin-3-yl)-acetic acid ethyl ester (14e)

The product was purified by column chromatography on silica gel (CH_2Cl_2/CH_3OH 9.5:0.5). Yield 55%, white solid; mp 290–291 °C; ^{1}H NMR (DMSO-d_6, 400 MHz): δ (ppm) 1.20 (t, 3H, J = 7.6), 2.30 (s, 3H), 4.15 (q, 2H, J = 7.6), 4.60 (s, 2H), 5.15 (s, 2H), 7.20–7.40 (m, 6H), 12.00 (br s, 1H).

4.1.32. 1-Benzyl-3-(2-dimethylamino-ethyl)-7-methyl-1*H*,8*H*-imidazo[2,1-*f*]purine-2,4-dione (14f)

The product was purified by column chromatography on silica gel (CH_2Cl_2/CH_3OH 9:1). Yield 80%, white solid; mp 245 °C; ^{1}H NMR (DMSO-d_6, 400 MHz): δ (ppm) 2.19 (s, 6H), 2.23 (s, 3H), 2.40 (t, 2H, J = 7.3), 4.00 (t, 2H, J = 7.3), 5.20 (s, 2H), 7.20–7.40 (m, 6H), 12.00 (br s, 1H).

4.1.33. General procedure for the preparation of 8-substituted-7-methyl-1*H*,8*H*-imidazo[2,1-*f*]purine-2,4-dione derivatives (15a–c)

A mixture of **3** (0.36 mmol) or **10** (0.36 mmol), triphenylphosphine (0.36 mmol) and the appropriate amine (0.43 mmol) in anhydrous THF (3 mL), was stirred at room temperature under argon atmosphere while a solution of diethyazodicarboxylate (0.36 mmol) in THF was added dropwise. After 1 h at room temperature, the solvent was evaporated and the residue partitioned between EtOAc (20 mL) and H_2O (2× 10 mL). The organic phase was dried on Na_2SO_4, filtered and the solvent was evaporated under vacuum till dryness.

4.1.34. 1-Benzyl-8-(2-hydroxy-1-methyl-ethyl)-7-methyl-1*H*,8*H*-imidazo[2,1-*f*]purine-2,4-dione (15a)

The product was purified by column chromatography on silica gel (CH_2Cl_2/CH_3OH 9.5:0.5). Yield 70%, white solid; mp 251–253 °C; ^{1}H NMR (DMSO-d_6, 200 MHz): δ (ppm) 1.50 (d, 3H, J = 6.8), 2.29 (s, 3H), 3.80 (m, 1H), 3.90 (m, 1H), 4.30 (m, 1H), 4.98 (bt, 1H), 5.09 (s, 2H), 7.26–7.38 (m, 6H), 10.91 (s, 1H).

4.1.35. 1-Benzyl-8-ethyl-7-methyl-1*H*,8*H*-imidazo[2,1-*f*]purine-2,4-dione (15b)

Il prodotto è stato The product was purified by column chromatography on silica gel (CH_2Cl_2/CH_3OH 9.9:0.1). Yield 50%, white solid; mp >300 °C; ^{1}H NMR (DMSO-d_6, 200 MHz): δ (ppm) 1.27 (t, 3H, J = 7.4), 2.26 (s, 3H), 3.98 (q, 2H, J = 7.4), 5.07 (s, 2H), 7.26–7.29 (m, 6H), 10.91 (s, 1H).

4.1.36. 1-Benzyl-8-ethyl-7-methyl-3-propyl-1*H*,8*H*-imidazo[2,1-*f*]-purine-2,4-dione (15c)

The product was purified by column chromatography on silica gel (CH_2Cl_2/CH_3OH 9.9:0.1). Yield 55%, white solid; mp 190 °C; ^{1}H NMR (DMSO-d_6, 200 MHz): δ (ppm) 0.84 (t, 3H, J = 7.3), 1.31 (t, 3H, J = 7.4), 1.53 (m, 2H), 2.32 (s, 3H), 3.83 (m, 2H), 4.01 (m, 2H), 5.18 (s, 2H), 7.27–7.33 (m, 6H).

4.1.37. General procedure for the preparation of 1,3-dialkyl-3,7-dihydro-purine-2,6-dione derivatives (17a–b)

A solution of 5,6-diamino-1,3-dialkyl-1H-pyrimidine-2,4-dione derivatives (**16a–b**) (3.28 mmol) were dissolved in formic acid (15 mL) and the resultant violet solution was refluxed for 1 h. The excess of acid was evaporated to obtain a yellow residue which was dissolved in a 1:1 mixture of EtOH–10% aqueous NaOH. The reaction mixture was refluxed for 1 h then the solvents were concentrated to half-volume. The products were precipitated by acidifying with 10% HCl, filtered and washed with cold water.

4.1.38. 1,3-Dipropyl-3,7-dihydro-purine-2,6-dione (17a)

Crystallization from ethanol gave the desired product as a pale yellow solid: 95% yield; mp 205 °C; ^{1}H NMR ($CDCl_3$, 200 MHz): δ 0.98 (t, 6H, J = 7.6), 1.67–1.88 (m, 4H), 4.03–4.16 (m, 4H), 7.81 (s, 1H), 12.98 (br s, 1H).

4.1.39. 1,3-Diisobutyl-3,7-dihydro-purine-2,6-dione (17b)

Crystallization from ethanol gave the desired product as a pale yellow solid: 90% yield; mp 194 °C; ^{1}H NMR (DMSO-d_6, 200 MHz): δ 0.84 (m, 12H), 1.90–2.20 (m, 2H), 3.73 (m, 4H), 7.79 (s, 1H), 13.00 (br s, 1H).

4.1.40. General procedure for the preparation of 1,3-dialkyl-8-bromo-3,7-dihydro-purine-2,6-dione derivatives (18a–b)

A solution of the appropriate 1,3-dialkyl-3,7-dihydro-purine-2,6-dione derivative (**17a–b**) (2.82 mmol) and sodium acetate (2.82 mmol) in acetic acid (15 mL) was warmed at 45 °C under stirring. To the mixture 0.15 mL of bromine (2.82 mmol) were added dropwise. After 1 h at 45 °C the solvent was evaporated, the residue suspended with water and extracted with EtOAc (3× 100 mL). The organic layers were dried with anhydrous sodium sulphate and evaporated to dryness.

4.1.41. 1,3-Dipropyl-8-bromo-3,7-dihydro-purine-2,6-dione (18a)

Crystallization from EtOH gave the desired product as a white solid: 70% yield; mp 193 °C; ^{1}H NMR ($CDCl_3$, 200 MHz): δ 0.88 (t, 6H, J = 7.6), 1.65–1.85 (m, 4H), 4.00–4.15 (m, 4H), 13.33 (br s, 1H).

4.1.42. 1,3-Diisobutyl-8-bromo-3,7-dihydro-purine-2,6-dione (18b)

Crystallization from EtOH gave the desired product as a white solid: 80% yield; mp 205–207 °C; ^{1}H NMR (DMSO-d_6, 200 MHz): δ 0.82 (m, 12H), 1.8–2.10 (m, 2H), 3.73 (m, 4H), 13.20 (br s, 1H).

4.1.43. 1,3-Dipropyl-8-bromo-7-(2-oxo-2-phenyl-ethyl)-3,7-dihydro-purine-2,6-dione (19a)

The product was synthesised according to the general alkylation procedure at the N^7-position described for the preparation of compound **10**, using α-bromoacetophenone as alkylating agent, and finally purified by crystallisation from EtOH: pale yellow solid; 70% yield; mp 160–161 °C; ^{1}H NMR ($CDCl_3$, 200 MHz): δ *0.87–1.03* (m, 6H), 1.57–1.84 (m, 4H), 3.85–3.92 (m, 2H), 4.02–4.10 (m, 2H), 5.84 (s, 2H), 7.51–7.68 (m, 3H), 7.99–8.05 (m, 2H).

4.1.44. 1,3-Diisobutyl-8-bromo-7-(2-oxo-2-phenyl-ethyl)-3,7-dihydro-purine-2,6-dione (19b)

The product was synthesised according to the general alkylation procedure at the N^7-position described for the preparation of compound **10**, using α-bromoacetophenone as alkylating agent, and finally purified by crystallisation from EtOH: pale yellow solid; 75% yield; mp 178–181 °C; ^{1}H NMR ($CDCl_3$, 200 MHz): δ *0.86–0.98* (m, 12H), 2.10 (m, 1H), 2.30 (m, 1H), 3.78 (d, 2H, J = 7.6), 3.93 (d, 2H, J = 7.6), 5.84 (s, 2H), 7.51–7.68 (m, 3H), 7.99–8.04 (m, 2H).

4.1.45. 1,3-Dipropyl-7-phenyl-1*H*,8*H*-imidazo[2,1-*f*]purine-2,4-dione (20a)

The product was synthesised according to the general cyclisation procedure described for the preparation of compound **6a–c, 12, 13, 14a–f** and finally purified by column chromatography on silica gel eluting with a 3:2 mixture of light petroleum–EtOAc: white solid; 50% yield; mp 249–250 °C; ^{1}H NMR (DMSO-d_6, 200 MHz): δ 0.87 (m, 6H), 1.40–1.80 (m, 4H), 3.80–4.05 (m, 4H), 7.30–7.60 (m, 3H), 7.80 (m, 2H), 8.10 (s, 1H), 13.00 (br s, 1H).

4.1.46. 1,3-Diisobutyl-7-phenyl-1*H*,8*H*-imidazo[2,1-*f*]purine-2,4-dione (20b)

The product was synthesised according to the general cyclisation procedure described for the preparation of compound **6a–c, 12, 13, 14a–f** and finally purified by column chromatography on silica gel eluting with a 7:3 mixture of light petroleum–EtOAc: white solid; 60% yield; mp 170 °C; ^{1}H NMR (DMSO-d_6, 200 MHz): δ 0.87 (m, 12H), 2.00–2.30 (m, 2H), 3.70–3.90 (m, 4H), 7.35–7.50 (m, 3H), 7.80 (m, 2H), 8.10 (s, 1H), 13.00 (br s, 1H).

4.1.47. 1,3-Dimethyl-8-amino-3,7-dihydro-purine-2,6-dione (22)

To a mixture of 8-nitro-theophylline (**21**, 1 g, 4.44 mmol) in 20 mL of methanol and hydrazine monohydrate (1 mL) was added 10% C/Pd (200 mg) and the reaction was refluxed until the yellow colour disappeared. 5% NaOH solution (5 mL) was added to the reaction mixture and the suspension was filtered through Celite. The filtrate was concentrated to half-volume and finally acidified with acetic acid to precipitate the product as a white solid. The precipitate was washed with water and dried under vacuum: white solid; 80% yield; mp >300 °C; ^{1}H NMR (DMSO-d_6, 200 MHz): δ 3.17 (s, 3H), 3.33 (s, 3H), 6.52 (s, 2H), 11.17 (br s, 1H).

4.1.48. 1,3-Dimethyl-8-amino-7-(2-oxo-2-phenyl-ethyl)-3,7-dihydro-purine-2,6-dione (23a)

The product was synthesised according to the general alkylation procedure at the N^7-position described for the preparation of compound **10**, using a-bromoacetphenone as alkylating agent, and purified by crystallization from EtOH. White solid: 80% yield; mp 248–250 °C; ^{1}H NMR (DMSO-d_6, 200 MHz): δ 3.10 (s, 3H), 3.36 (s, 3H), 5.60 (s, 2H), 7.00 (s, 2H), 7.70 (m, 5H).

4.1.49. 1,3-Dimethyl-8-amino-7-(2-oxo-propyl)-3,7-dihydro-purine-2,6-dione (23b)

The product was synthesised according to the general alkylation procedure at the N^7-position described for the preparation of compounds **5a–c**. Crystallization from EtOH gave the desired product as a white solid: 80% yield; mp 230–232 °C; ^{1}H NMR (DMSO-d_6, 200 MHz): δ 2.50 (s, 3H), 3.20 (s, 3H), 3.50 (s, 3H), 5.20 (s, 2H), 7.00 (s, 2H).

4.1.50. General procedure for the preparation of 1,3-dimethyl-7-substituted-1*H*,8*H*-imidazo[2,1-*f*]purine-2,4-dione derivatives (24a–b)

The appropriate 1,3-dimethyl-8-amino-7-(2-oxo-alkyl)-3,7-dihydro-purine-2,6-dione derivatives **23a–b** (0.3 mmol) was heated at reflux in acetic acid (5 mL) for 4 h. The solvent was evaporated and the residue crystallized from the opportune solvents.

4.1.51. 1,3-Dimethyl-7-phenyl-1*H*,8*H*-imidazo[2,1-*f*]purine-2,4-dione (24a)

Crystallization from DMF gave the desired product as a white solid: 70% yield; mp 283–285 °C; ^{1}H NMR (DMSO-d_6, 200 MHz): δ 3.24 (s, 3H), 3.44 (s, 3H), 7.42 (m, 3H), 7.78 (m, 2H), 8.07 (s, 1H), 12.90 (br s, 1H).

4.1.52. 1,3,7-Trimethyl-1*H*,8*H*-imidazo[2,1-*f*]purine-2,4-dione (24b)

Crystallization from DMF gave the desired product as a white solid: 60% yield; mp 247–248 °C; ^{1}H NMR (DMSO-d_6, 200 MHz): δ 2.66 (s, 3H), 3.22 (s, 3H), 3.41 (s, 3H); 7.23 (s, 1H), 12.20 (br s, 1H).

4.2. Biology experiments

4.2.1. CHO membranes preparation

The human A_1, A_{2A}, A_{2B} and A_3 receptors has been transfected in CHO cells according with the method previously described.[53] The cells were grown adherently and maintained in Dulbecco's modified Eagle's medium with nutrient mixture F12 (DMEM/F12) without nucleosides, containing 10% foetal calf serum, penicillin (100 U/ml), streptomycin (100 μg/ml), L-glutamine (2 mM) and Geneticin (G418, 0,2 mg/ml) at 37 °C in 5% CO_2/95% air. Cells were split 2 or 3 times weekly at a ratio between 1:5 and 1:20. For membrane preparation the culture medium was removed and the cells were washed with PBS and scraped off T75 flasks in ice-cold hypotonic buffer (5 mM Tris–HCl, 2 mM EDTA, pH 7.4). The cell suspension was homogenized with Polytron and the homogenate was spun for 10 min at 1000*g*. The supernatant was then centrifuged for 30 min at 100,000*g*. The membrane pellet was suspended in 50 mM Tris–HCl buffer pH 7.4 (for A_3 adenosine receptors: 50 mM Tris–HCl, 10 mM $MgCl_2$, 1 mM EDTA) and incubated with 3 UI/ml of adenosine deaminase for 30 min at 37 °C. Then the cell suspension was frozen at −80 °C.

4.2.2. Human cloned A_1, A_{2A} and A_3 adenosine receptor binding assay

All synthesized compounds have been tested for their affinity at human A_1, A_{2A} and A_3 adenosine receptors. Displacement experiments of [^{3}H]-DPCPX to CHO cells transfected with the human recombinant A_1 adenosine receptor were performed for 120 min at 25 °C in 0.2 ml of 50 mM Tris–HCl buffer, pH 7.4, containing 1 nM [^{3}H]-DPCPX, diluted membranes (50 μg of protein/assay) and at least 6–8 different concentrations of antagonists studied. Non-specific binding was determined in the presence of 10 μM of CHA and this was always ≤10% of the total binding.[54]

Binding of [^{3}H]-ZM 241385 to CHO cells transfected with the human recombinant A_{2A} adenosine receptors (50 μg of protein/assay) was performed using 0.2 ml of 50 mM Tris–HCl buffer, 10 mM $MgCl_2$, pH 7.4, and at least 6–8 different concentrations of antagonists studied for an incubation time of 60 min at 4 °C. Non-specific binding was determined in the presence of 1 μM ZM 241385 and was about 20% of total binding.[55]

Binding of [^{3}H]-MRE 3008F20 to CHO cells transfected with the human recombinant A_3 adenosine receptors was performed performed as previously described.[56] Competition experiments were carried out in duplicate in a final volume of 250 μl in test tubes containing 1 nM [^{3}H]-MRE 3008F20, 50 mM Tris–HCl buffer, 10 mM $MgCl_2$, 1 mM EDTA, pH 7.4, and 100 μl of diluted membranes (50 μg of protein/assay) and at least 6–8 different concentrations of examined ligands for 120 min at 4 °C. Non-specific binding was defined as binding in the presence of 1 μM MRE 3008F20 and was about 25% of total binding. Bound and free radioactivities were separated by filtering the assay mixture through Whatman GF/B glass fibre which were washed three times with ice-cold buffer. Filter bound radioactivity was measured by scintillation spectrometry (LS-1800 Beckman) after addition of Aquassure liquid.

4.2.3. Measurement of cyclic AMP levels in CHO cells transfected with human A_{2B} adenosine receptors

CHO cells transfected with human A_{2B} adenosine receptors were washed with phosphate-buffered saline, diluted trypsine and centrifuged for 10 min at 200*g*. The pellet containing the CHO cells (1×10^6 cells /assay) was suspended in 0.5 ml of incubation mixture (mM): NaCl 15, KCl 0.27, NaH_2PO_4 0.037, $MgSO_4$ 0.1, $CaCl_2$ 0.1, Hepes 0.01, $MgCl_2$ 1, glucose 0.5, pH 7.4, at 37 °C, 2 IU/ml adenosine deaminase and 4-(3-butoxy-4-methoxybenzyl)-2-imidazolidinone (Ro 20–1724) as phosphodiesterase inhibitor and preincubated for 10 min in a shaking bath at 37 °C. The potencies of antagonists studied versus hA_{2B} adenosine receptors were determined by antagonism of NECA (100 nM)-induced stimulation of cyclic AMP levels. The reaction was terminated by the addition of cold 6% trichloroacetic acid (TCA). The TCA suspension was centrifuged at 2000 g for 10 min at 4 °C and the supernatant was extracted four times with water saturated diethyl ether. The final aqueous solution was tested for cyclic AMP levels by a competition protein binding assay. Samples of cyclic AMP standard (0–10 pmol) were added to each test tube containing the incubation buffer (trizma base 0.1 M, aminophylline 8.0 mM, 2-mercaptoethanol 6.0 mM, pH 7.4) and [^{3}H] cyclic AMP in a total volume of 0.5 ml. The binding protein previously prepared from beef adrenals, was added to the samples previously incubated at 4 °C for 150 min, and after the addition of charcoal were centrifuged at 2000*g* for 10 min. The clear supernatant was counted in a LS-1800 Beckman scintillation counter.

4.2.4. Data analysis

The protein concentration was determined according to a Bio-Rad method[57] with bovine albumin as a standard reference. Inhibitory binding constants, K_i values, were calculated from those of IC_{50} according to Cheng & Prusoff equation[58] $K_i = IC_{50}/(1+[C^*]/K_D^*)$, where $[C^*]$ is the concentration of the radioligand and K_D^* its dissociation constant. A weighted non-linear least-squares curve fitting program LIGAND[59] was also used for computer analysis of inhibition experiments. Potency values (IC_{50}) obtained in cyclic AMP assays were calculated by non-linear regression analysis using the equation for a sigmoid concentration-response curve (Graph PAD Prism, San Diego, CA, USA). Affinity values are expressed as geometric mean, with 95% or 99% confidence limits in parentheses and IC_{50} values are expressed as the arithmetic means ± SEM.

4.3. Receptor modeling

Molecular mechanics (MM) and molecular dynamics (MD) calculations were performed using the AMBER force field as implemented in the MacroModel software package,[60] using a "distance-dependent" dielectric constant of 4.0. Electrostatic charges for compound **1a** were calculated with RHF/AM1 semi-empirical calculation and RESP program.[61]

All MM minimizations were performed with conjugate gradient or steepest descent as minimizers and a threshold value of 0.05 kJ/

Å mol as the convergence criterion. The temperature was set at 300 K and the time step was 1.0 fs in MD simulations.

As A_3 receptor starting structure was used the one reported in our previous paper (MODEL 1),[48] compound **1a** was docked inside the receptor by means of AUTODOCK 3.0.[47]

The regions of interest used by AUTODOCK were defined by considering residue N250 as the central group; in particular, a grid of 40, 44, and 40 points in the *x*, *y*, and *z* directions was constructed centred on the centre of the mass of N250. A grid spacing of 0.375 Å and a distance-dependent function of the dielectric constant were used for the energetic map calculations.

AUTODOCK TOOLS[62] was used to identify the torsion angles in the ligands, add the solvent model and assign partial atomic charges (Gasteiger for the ligands and Kollman for the receptors).

Using the Lamarckian Genetic Algorithm, the compounds were subjected to 100 runs of the AUTODOCK search, in which the default values of the other parameters were used.

Cluster analysis was performed on the docked results using an RMS tolerance of 1.0 Å and the best docked structure was taken into consideration for further analysis.

The A3–**1a** complex was refined using the previously reported procedure.[48] It mainly consisted of a total of 400 ps of MD in which all the alpha carbons of the TM, and the main ligand-receptor interactions were constrained during the trajectory by means of decreasing the force constants. More in detail, an initial restraint with a force constant of 10 Kcal/mol Å^2 was applied on the alpha carbons. This force constant decreased during the whole MD and in the last 200 ps a value of 0.1 kcal/mol Å^2 was applied. As regards the H bond ligand-receptor interactions, a restraint of 50 kcal/mol Å^2 was applied on the H bond between N250 and the carbonyl of the ligand. At the end of the MD simulation, three steps of minimization were applied on the average structure obtained during the last 100 ps of the MD run. During these three steps a restraint of 0.1 kcal/mol Å^2 was applied on the alpha carbons, while with regard to the ligand-N250H bond, in the first two steps a restraint of respectively 25 and 10 Kcal/mol Å^2 was applied and in the last one the restraint was removed.

4.4. Docking studies

The ligands were built through Maestro program and were then subjected to a conformational search of 500 steps in a water environment (using the Generalized-Born/Surface-Area model) by means of Macromodel. The algorithm used was the Montecarlo method with the MMFFs forcefield and a distance-dependent dielectric constant of 1.0. The ligands were then minimized using the conjugated gradient method until a convergence value of 0.05 kcal/Å mol, using the same forcefield and parameters as for the conformational search.

Then the so minimized ligands were docked in the A3 receptor by means of AUTODOCK 3.0[47] using the procedure described above.

Cluster analysis was performed on the docked results using an RMS tolerance of 1.0 Å and the best docked structure was taken into consideration, furthermore for most of the ligands the first cluster corresponded also to the most populated one.

4.5. 3D-QSAR study

Before construction of the 3D-QSAR model, the binding free energy calculated for each ligand-AT1 complex by means of the AUTODOCK scoring function was correlated with the experimental antagonist affinity, but the quadratic correlation (R^2) showed a low value ($R^2 < 0.4$).

For each ligand, the best docked structure was chosen and this receptor-based alignment was used for further studies. A second 3D-QSAR study was developed aligning the ligands on the basis of their central scaffold. The GOLPE program[52] was used to define the 3D-QSAR models, using GRID interaction fields[63] as descriptors (see below). Given the low number of ligands (34 compounds) the training set was composed by all the compounds and the 3D-QSAR model was validated through the correlation coefficient (r^2), predictive correlation coefficient (q^2) and cross-validated standard deviation of errors of prediction ($SDEP_{CV}$), did not taking into account any external test set. Inactive compounds were also included in the training set, to which was arbitrarily assigned a K_i value equal to 1000 nM. The GRID program[63] was used to describe the previously superimposed molecular structure. Interaction energies between selected probes and each molecule were calculated using a grid spacing of 1 Å. In order to evaluate the lipophilic, H bond acceptor and donor properties of the ligands the C3 (methyl), O (carbonylic oxygen) and N2= (sp^2 amine cation) probes were used.

The MIFs of the training set were imported into GOLPE, variable selection was operated by zeroing values with absolute values smaller than 0.06 kcal/mol and removing variables with a standard deviation below 0.1. Moreover, variables which exhibited only two values and had a skewed distribution were also removed.

The smart region definition (SRD) algorithm[64] was applied with 10% of the active variables as the number of seed (selected in the PLS weights space), a critical distance cutoff of 2.5 Å, and a collapsing distance cutoff of 4.0 Å. The groups were then used in the Fractional Factorial Design (FFD) procedure. FFD selection was applied, until the r^2 and q^2 values did not increase significantly, using the cross-validation routine with five random sets of compounds.

Acknowledgements

We thank Prof. Karl-Norbert Klotz for cDNA encoding the human adenosine receptors and Prof. Gabriele Cruciani and Prof. Sergio Clementi (Molecular Discovery and MIA srl) for the use of the GOLPE program in their chemometric laboratory (University of Perugia, Italy) and for having provided the GRID program.

Supplementary data

Supplementary data associated with this article can be found, in the online version, at doi:10.1016/j.bmc.2008.10.049.

References and notes

1. Fredholm, B. B.; Arslan, G.; Halldner, L.; Kull, B.; Schulte, G.; Wasserman, W. *Naunyn-Schmied. Arch. Pharm.* **2000**, *362*, 364–374.
2. Williams, M.; Jarvis, M. F. *Biochem. Pharmacol.* **2000**, *59*, 1173.
3. Fredholm, B. B.; Ijzerman, A. P.; Jacobson, K. A.; Klotz, K-N.; Linden, J. *Pharm. Rev.* **2001**, *53*, 527.
4. Baharav, E.; Bar-Yehuda, S.; Madi, L.; Silberman, D.; Rath-Wolfson, L.; Halpren, M.; Ochaion, A.; Weinberger, A.; Fishman, P. *J. Rheumatol.* **2005**, *32*, 469.
5. Jacobson, K. A.; Kim, H. O.; Siddiqui, S. M.; Olah, M. E.; Stiles, G. L.; Von Lubitz, D. K. J. E. *Drugs Future* **1995**, *20*, 689.
6. Kohno, Y.; Ji, X. D.; Mawhorter, S. D.; Koshiba, M.; Jacobson, K. A. *Blood* **1996**, *88*, 3569.
7. Jacobson, K. A. *Trends. Pharmacol. Sci.* **1998**, *19*, 184.
8. Von Lubitz, D. K. J. E.; Lin, R. C. S.; Popik, P.; Carter, M. F.; Jacobson, K. A. *Eur. J. Pharmacol.* **1994**, *263*, 59.
9. Rivo, J.; Zeira, E.; Galun, E.; Matot, I. *Anesthesiology* **2004**, *101*, 1153.
10. Brown, R. A.; Spina, D.; Page, C. P. *Br. J. Pharmacol.* **2008**, *153*, S446.
11. Marx, D.; Ezeamuzie, C. I.; Nieber, K.; Szelenyi, I. *Drug News Perspect.* **2001**, *14*, 89.
12. Okamura, T.; Kurogi, Y.; Hashimoto, K.; Sato, S.; Nishikawa, H.; Kiryu, K.; Nagao, Y. *Bioorg. Med. Chem. Lett.* **2004**, *14*, 3775.
13. Schlotzer-Schrehardt, U.; Zenkel, M.; Decking, U.; Haubs, D.; Kruse, F. E.; Junemann, A.; Coca-Prados, M.; Naumann, G. O. *Invest. Ophthalmol. Vis. Sci.* **2005**, *46*, 2023.
14. Avila, M. Y.; Stone, R. A.; Civan, M. M. *Invest. Ophthalmol. Vis. Sci.* **2002**, *43*, 3021.
15. Gessi, S.; Varani, K.; Merighi, S.; Cattabriga, E.; Avitabile, A.; Gavioli, R.; Fortini, C.; Leung, E.; Mac Lennan, S.; Borea, P. A. *Mol. Pharmacol.* **2004**, *65*, 711.
16. Ohana, G.; Bar-yehuda, S.; Barer, F.; Fishman, P. *J. Cell Phys.* **2001**, *186*, 19.
17. Baraldi, P. G.; Borea, P. A. *Trends Pharm. Sci.* **2000**, *21*, 456.

18. Merighi, S.; Mirandola, P.; Varani, K.; Gessi, S.; Leung, E.; Baraldi, P. G.; Tabrizi, M. A.; Borea, P. A. *Pharmacol. Ther.* **2003**, *1001*, 31.
19. Fishman, P.; Bar-Yehuda, S.; Barer, F.; Ohana, G. *Drug. Dev. Res.* **2000**, *50*, 101.
20. Madi, L.; Ochaion, A.; Rath-Wolfson, L.; Bar-Yehuda, S.; Erlanger, A.; Ohana, G.; Harish, A.; Merimski, O.; Barer, F.; Fishman, P. *Clin. Cancer Res.* **2004**, *10*, 4472.
21. Gessi, S.; Varani, K.; Merighi, S.; Morelli, A.; Ferrari, D.; Leung, E.; Baraldi, P. G.; Spalluto, G.; Borea, P. A. *Br. J. Pharmacol.* **2001**, *134*, 116.
22. Merighi, S.; Varani, K.; Gessi, S.; Cattabriga, E.; Iannotta, V.; Uloglou, C.; Leung, E.; Borea, P. A. *Br. J. Pharmacol.* **2001**, *134*, 1215.
23. Borea, P. A.; Baraldi, P. G.; Chen, S.F.; Leung, E. PCT Int. Appl. **2003**, WO 2004000224.
24. Gessi, S.; Cattabriga, E.; Avitabile, A.; Gafa', R.; Lanza, G.; Cavazzini, L.; Bianchi, N.; Gambari, Roberto.; Feo, Carlo.; Liboni, A.; Gullini, S.; Leung, E.; Mac-Lennan, S.; Borea, P. A. *Clin. Canc. Res.* **2004**, *10*, 5895.
25. Baraldi, P. G.; Tabrizi, M. A.; Fruttarolo, F.; Bovero, A.; Avitabile, B.; Preti, D.; Romagnoli, R.; Merighi, S.; Gessi, S.; Varani, K.; Borea, P. A. *Drug Dev. Res.* **2003**, *58*, 315.
26. Baraldi, P. G.; Cacciari, B.; Romagnoli, R.; Merighi, S.; Varani, K.; Borea, P. A.; Spalluto, G. *Med. Res. Rev.* **2000**, *20*, 103.
27. Muller, C. E. *Curr. Top. Med. Chem.* **2003**, *3*, 445.
28. Okamura, T.; Kurogi, Y.; Nishikawa, H.; Hashimoto, K.; Fujiwara, H.; Nagao, Y. *J. Med. Chem.* **2002**, *45*, 3703.
29. Colotta, V.; Catarzi, D.; Varano, F.; Cecchi, L.; Filacchioni, G.; Martini, C.; Trincavelli, L.; Lucacchini, A. *J. Med. Chem.* **2000**, *43*, 1158.
30. Colotta, V.; Catarzi, D.; Varano, F.; Calabri, F. R.; Lenzi, O.; Filacchioni, G.; Martini, C.; Trincavelli, L.; Deflorian, F.; Moro, S. *J. Med. Chem.* **2004**, *47*, 3580.
31. Jung, K. Y.; Kim, S. K.; Gao, Z. G.; Gross, A. S.; Melman, N.; Jacobson, K. A.; Kim, Y. C. *Bioorg. Med. Chem.* **2004**, *12*, 613.
32. Press, N. J.; Keller, T. H.; Tranter, P.; Beer, D.; Jones, K.; Faessler, A.; Heng, R.; Lewis, C.; Howe, T.; Gedeck, P.; Mazzoni, L.; Fozard, J. R. *Curr. Top. Med. Chem.* **2004**, *4*, 863.
33. Muller, C. E.; Thorand, M.; Qurishi, R.; Diekmann, M.; Jacobson, K. A.; Padgett, W. L.; Daly, J. W. *J. Med. Chem.* **2002**, *45*, 3440.
34. Priego, E. M.; von Frijtag Drabbe Kuenzel, J.; Ijzerman, A. P.; Camarasa, M. J.; Perez-Perez, M. J. *J. Med. Chem.* **2002**, *45*, 3337.
35. Colotta, V.; Catarzi, D.; Varano, F.; Capelli, F.; Lenzi, O.; Filacchioni, G.; Martini, C.; Trincavelli, L.; Ciampi, O.; Pugliese, A. M.; Pedata, F.; Schiesaro, A.; Morizzo, E.; Moro, S. *J. Med. Chem.* **2007**, *50*, 4061.
36. Baraldi, P. G.; Tabrizi, M. A.; Preti, D.; Bovero, A.; Fruttarolo, F.; Romagnoli, R.; Zaid, N. A.; Moorman, A. R.; Varani, K.; Borea, P. A. *J. Med. Chem.* **2005**, *48*, 5001.
37. Gao, Z. G.; Joshi, B. V.; Klutz, A. M.; Kim, S. K.; Lee, H. W.; Kim, H. O.; Jeong, L. S.; Jacobson, K. A. *Bioorg. Med. Chem. Lett.* **2006**, *16*, 596.
38. Jeong, L. S.; Choe, S.; Gunaga, P.; Kim, H. O.; Lee, H. W.; Lee, S. K.; Tosh, D. K.; Patel, A.; Palaniappan, K. K.; Gao, Z. G.; Jacobson, K. A.; Moon, H. R. *J. Med. Chem.* **2007**, *50*, 3159.
39. Jeong, L. S.; Lee, H. W.; Kim, H. O.; Tosh, D. K.; Pal, S.; Choi, W. J.; Gao, Z. G.; Patel, A. R.; Williams, W.; Jacobson, K. A.; Kim, H. D. *Bioorg. Med. Chem. Lett.* **2008**, *18*, 1612.
40. Drabczyńska, A.; Schumacher, B.; Müller, C. E.; Karolak-Wojciechowska, J.; Michalak, B.; Pękala, E.; Kieć-Kononowicz, K. *Eur. J. Med. Chem.* **2003**, *38*, 397.
41. Baraldi, P. G.; Abdel, Z. N.; Fruttarolo, F.; Tabrizi, A. M.; Nuñez, M.; Spalluto, G.; Romagnoli, R. *Synthesis* **2001**, *5*, 773.
42. Baraldi, P. G.; Preti, D.; Tabrizi, M. A.; Fruttarolo, F.; Romagnoli, R.; Zaid, N. A.; Moorman, A. R.; Merighi, S.; Varani, K.; Borea, P. A. *J. Med. Chem.* **2005**, *48*, 4697.
43. Kramer, G. L.; Garst, J. E.; Mitchel, S. S.; Wells, J. N. *Biochemistry* **1977**, *16*, 3316.
44. Holschbach, M. H.; Fein, T.; Krummeich, C.; Lewis, R. G.; Wutz, W.; Schwabe, U.; Unterlugauer, D.; Olsson, R. A. *J. Med. Chem.* **1998**, *41*, 555.
45. Papesch, V.; Schroeder, E. F. *J. Org. Chem.* **1951**, *16*, 1879.
46. Mosselhi, A.; Pfleidered, W. Purines. XIV. *J. Heterocycl. Chem.* **1993**, *30*, 1221.
47. Morris, G. M.; Goodsell, D. S.; Halliday, R. S.; Huey, R.; Hart, W. E.; Belew, R. K.; Olson, A. J. *J. Comp. Chem.* **1998**, *19*, 1639.
48. Tafi, A.; Bernardini, C.; Botta, M.; Corelli, F.; Andreini, M.; Martinelli, A.; Ortore, G.; Baraldi, P. G.; Fruttarolo, F.; Borea, P. A.; Tuccinardi, T. *J. Med. Chem.* **2006**, *49*, 4085.
49. Gao, Z. G.; Kim, S. K.; Biadatti, T.; Chen, W.; Lee, K.; Barak, D.; Kim, S. G.; Johnson, C. R.; Jacobson, K. A. *J. Med. Chem.* **2002**, *45*, 4471.
50. Gao, Z. G.; Chen, A.; Barak, D.; Kim, S. K.; Muller, C. E.; Jacobson, K. A. *J. Biol. Chem.* **2002**, *277*, 19056.
51. Manetti, F.; Schenone, S.; Bondavalli, F.; Brullo, C.; Bruno, O.; Ranise, A.; Mosti, L.; Menozzi, G.; Fossa, P.; Trincavelli, M. L.; Martini, C.; Martinelli, A.; Tintori, C.; Botta, M. *J. Med. Chem.* **2005**, *48*, 7172.
52. GOLPE 4.5. Multivariate Infometric Analysis Srl., Viale dei Castagni 16, Perugia, Italy, 1999.
53. Klotz, K. N.; Hessling, J.; Hegler, J.; Owman, C.; Kull, B.; Fredholm, B. B.; Lohse, M. J. *Naunyn-Schmied. Arch. Pharm.* **1998**, *357*, 1.
54. Borea, P. A.; Dalpiaz, A.; Varani, K.; Gessi, S.; Gilli, G. *Life Sci.* **1996**, *59*, 1373.
55. Borea, P. A.; Dalpiaz, A.; Varani, K.; Gessi, S.; Gilli, G. *Biochem. Pharmacol.* **1995**, *49*, 461.
56. Varani, K.; Merighi, S.; Gessi, S.; Klotz, K. N.; Leung, E.; Baraldi, P. G.; Cacciari, B.; Romagnoli, R.; Spalluto, G.; Borea, P. A. *Mol. Pharmacol.* **2000**, *57*, 968.
57. Bradford, M. M. *Anal. Biochem.* **1976**, *72*, 248.
58. Cheng, Y. C.; Prusoff, W. H. *Biochem. Pharmacol.* **1973**, *22*, 3099.
59. Munson, P. J.; Rodbard, D. *Anal. Biochem.* **1980**, *107*, 220.
60. *Macromodel*, ver. 8.5; Schrödinger Inc.: Portland, OR, 1999.
61. Pearlman, D. A.; Case, D.; Caldwell, J. W.; Ross, W. S.; Cheatham TE, I. I. I.; Ferguson, D. M.; Seibel, G. L.; Chandra Singh, U.; Weiner, P. K.; Kollman, P. A. *AMBER 41*; University of California, San Francisco: San Francisco, 1995.
62. http://www.scripps.edu/~sanner/python/adt.
63. Cruciani, G; Goodford, P. Copyright Molecular Discovery Ltd. 2001–2003 GREATER graphical interface for GRID version, 1.1.7 GRIB, UPF/IMIM, Barcelona (Spain). Available from: http://www.moldiscovery.com.
64. Pastor, M.; Cruciani, G.; Clementi, S. *J. Med. Chem.* **1997**, *40*, 1455.